Chapter 2
The Standard Model of Cosmology

2.1 Introduction

The standard model of cosmology encompasses our knowledge of the Universe as a whole. It has matured over the last century, consolidating its theoretical foundations with increasingly accurate observations. The main assumptions on which it rests are:

- On sufficiently large scales the Universe is homogeneous and isotropic (the *cosmological principle*).
- The energy content of the Universe is modelled in terms of cosmological fluids with constant equation of state: photons, baryons, neutrinos, cold dark matter and dark energy.
- The gravitational interactions between the cosmological fluids are described by Einstein's general relativity (GR).

Along with the above theoretical assumptions, the standard model of cosmology includes the fundamental observation that the Universe is expanding.

2.1.1 Summary of the Chapter

In this chapter we analyse these features in detail, starting with the cosmological principle in Sect. 2.2. The assumptions of isotropy and homogeneity lead to the formulation of the *FLRW* metric, which we introduce in Sect. 2.3. We derive the dynamic evolution of this metric in Sect. 2.4 by solving the Einstein equation; in particular, we find that the cosmic expansion is one of the solutions and is favoured by the measured abundances of the various species. The presence of a cosmic expansion, in turn, indicates that the primordial Universe was in a very hot and dense state where thermal equilibrium between the species was established. This prediction is spectacularly confirmed by the observation of a cosmic microwave background with a blackbody spectrum, which is the subject of Sect. 2.5. We conclude the chapter by

G.W. Pettinari, *The Intrinsic Bispectrum of the Cosmic Microwave Background*,
Springer Theses, DOI 10.1007/978-3-319-21882-3_2

discussing in Sect. 2.6 some important problems of the hot Big Bang scenario and one of the possible ways to solve them: the mechanism of cosmic inflation, a phase of accelerated expansion in the early Universe.

Note that in Sect. 2.6.4 we shall briefly discuss how non-linearities might arise during inflation that generate non-Gaussian signatures. The work described in this thesis is ultimately motivated by the quest to measure said non-Gaussianity.

2.2 The Cosmological Principle

The cosmological principle (CP) states that on sufficiently large scales the Universe is homogeneous and isotropic. *Homogeneity* means that different patches of the Universe have the same average physical properties. In particular, any cosmological fluid has the same energy density, pressure and temperature everywhere. *Isotropy* means that there are no preferred directions in the Universe. Any observer measuring a cosmological quantity—e.g. the photon flux or a galaxy count—in two different directions should find the same value.

Homogeneity does not imply isotropy. For example, a Universe filled with a homogeneous magnetic field is homogeneous but not isotropic. On the other hand, isotropy about one location does not guarantee homogeneity. The simplest case is given by an observer at the centre of an isotropic explosion, but there are other examples of inhomogeneous distributions that project isotropically on the sky of one observer [25]. However, isotropy about two locations does guarantee homogeneity and isotropy about all locations (Peacock [62, pp.65–67]).

The cosmological principle is spectacularly violated on small scales. Planets, stars and galaxies should not exist in a perfectly homogeneous Universe. However, when zooming out on scales larger than roughly $100\,\mathrm{h}^{-1}\,\mathrm{Mpc}$, where $1\mathrm{Mpc} = 3.086 \times 10^{22}\,\mathrm{m} = 3.262 \times 10^{6}\,\mathrm{ly}$ is roughly the average distance between two galaxies, the Universe does become smooth, as we detail in Sect. 2.2.1. This allows us to treat the dynamics of the cosmological fluids on the largest scales as if the Universe were perfectly homogeneous and isotropic. In this limit, the physics and the resulting equation are particularly simple, as discussed in Sect. 2.3.

The cosmological principle also allows us to define a universal time variable, the *cosmic time*, defined as the time measured by observers at rest with respect to the matter in their vicinity. The homogeneity of the Universe ensures that the clocks of these fundamental observers can be synchronised with respect to the evolution of the universal homogeneous density. We choose the zero of the cosmic time to coincide with the Big Bang, which we shall introduce in Sect. 2.4. As a consequence, the cosmic time is interpreted as the age of the Universe.

2.2.1 Validity of the Cosmological Principle

The cosmological principle is crucial in order to make sense of the Universe, as it allows us to give universal significance to our local measurements. Furthermore, as we shall see in Sect. 2.4, it leads to an elegant dynamical solution of Einstein's equations. When it was proposed , however, the cosmological principle was little more than a conjecture. As cosmological observations increased in number and accuracy, it was substantiated by more and more evidence. Nevertheless, the cosmological principle has not been proven unambiguously yet.

The main difficulty lies in the fact that it is impossible to observationally prove the homogeneity of the Universe without first assuming the Copernican principle, according to which we do not occupy a special position in the Universe.[1] The reason is that any observation has only access to our past light cone. Even worse, we cannot effectively move in cosmic time or space, so that we can only probe the past light cone of here and now. As a result, our observations mix time and space in such a way that we cannot tell the difference between an evolving homogeneous distribution of matter and an inhomogeneous one with a different time evolution [52].

If we accept the Copernican principle, however, the existence of isotropy in the observable Universe (that is, isotropy in the past light cone of Earth) would automatically imply the homogeneity of the whole Universe [26, 52]. Isotropy, contrary to homogeneity, is well established by many observations. The most relevant ones are the nearly perfect isotropy of the Cosmic Microwave Background [11], the isotropy of the X-ray background [71] and the isotropies of various source populations, e.g. radio galaxies [64]. The isotropy of the CMB also provides a good argument for homogeneity, since its angular distribution is linked to the three-dimensional fluctuations of the gravitational potential during recombination [84].

Not assuming the Copernican principle has two important consequences. First, the observed isotropy could not be used to infer homogeneity, not even in our local Universe. Secondly, observations would need to be interpreted in light of our special position. This is the case in the so-called void models, where the cosmological principle is assumed to be valid but our Galaxy sits close to the center of an underdense area which is radially inhomogeneous (the void). While some of these models have the benefit of removing the need for a cosmological constant by modifying the redshift-distance relationship (see, e.g., Refs. [55, 60, 80]), they fail to reproduce all the available observations at the same time [14, 17, 58, 83, 86, 88, 89]. For a review of other ways to test the Copernican principle, refer to Refs. [16, 35, 52].

A useful check for the homogeneity of the observable Universe consists in counting objects in a galaxy-survey in regions of increasing volume. In a homogeneous Universe, the mean density of galaxies in these regions should approach a constant value at a certain *homogeneity scale*. In order to look for this scale in the data, one needs to assume a cosmological model to convert the measured fluxes of galaxies to distances; hence it is more of a consistency check for homogeneous models rather

[1] This is also referred to as the *weak cosmological principle* by Ellis [26].

than a test of homogeneity. [2]He largest-volume measurement ($V \sim 1\,\mathrm{h}^{-3}\,\mathrm{Gpc}^3$) to date was performed by Scrimgeour et al. [72] using the blue galaxies of the WiggleZ survey [23]. They found homogeneity for scales larger than $70\,\mathrm{h}^{-1}$ Mpc, in agreement with what previously obtained by Hogg et al. [40] using large red galaxies,[3] and in disagreement with earlier results that suggested a fractal structure of the Universe [66, 79]. Interesting discussions about the scale of homogeneity and the fractal Universe can also be found in Refs. [19, 34]. For an observational test of homogeneity that relies only on the angular distances of galaxies, and is therefore less model-dependent, refer to Ref. [5].

2.3 The Expansion of the Universe

In the 1910s Vesto Slipher had noticed by measuring their light spectra that most of nearby galaxies—or *nebulae*, as they were called at the time—were quickly receding from us [75, 76]. In 1929, Edwin Hubble [41] independently confirmed that galaxies where receding and found a correlation between their radial velocity and their distance from us. This observation is encoded in *Hubble's law*, whereby there is a linear relationship between the radial speed with which a galaxy recedes from Earth and its distance to it:

$$v = H_0\, r\ . \tag{2.1}$$

The proportionality constant is now called *Hubble constant*.

If one assumes the cosmological principle, Hubble's law becomes universal: any two galaxies move away from each other with a speed proportional to the distance that separates them. In reality, the cosmological principle alone suffices to enforce the proportionality between distance and radial velocity. Isotropy enforces the radial motion, while homogeneity ensures that the recession velocity is proportional to the distance [36, 62]. However, the cosmological principle alone does not specify the sign of this proportionality, which Hubble found to be positive.

Hubble's discovery was soon linked to previous theoretical papers by Georges Lemaître [45, 46] and Alexander Friedmann [32]. In these pioneering works, the authors found dynamical solutions to Einstein equations where the Universe could expand indefinitely in a homogeneous manner. In this context, Hubble's law is the empirical consequence of a more fundamental concept: space itself is expanding. The apparent recession of galaxies is just one manifestation of the expansion of the Universe, and H_0 represents the homogeneous expansion rate.[4] In the expanding

[2]T.

[3]As a comparison consider that the disk of our Galaxy, the Milky Way, which is an average galaxy, measures just around 30 kpc.

[4]It is sometimes thought that Hubble discovered the expansion of the Universe in his 1929 paper. This was not the case, as the first connection to Lemaître and Friedmann works was made in 1930

Universe picture, the receding galaxies are not thought as projectiles shooting away through space, but as objects at rest in expanding space. Similarly, the recession speed is not the speed of something moving through space, but of space itself; it is not a local phenomenon and this is why it can exceed the speed of light without changing the causal structure of space-time [36].

The value of H_0 cannot be predicted by theoretical means: only observation can pin it down. Since distance measurements are subject to high uncertainty, it is customary to parametrize the Hubble constant by means of the pure number h:

$$H_0 \equiv 100\ \mathrm{h}\ \frac{\mathrm{km/s}}{\mathrm{Mpc}} \tag{2.2}$$

$$= \frac{h}{9.77\mathrm{Gyr}} \tag{2.3}$$

$$= \frac{h}{4.69 \times 10^{41}}\ \mathrm{GeV} \qquad (\text{assuming } \hbar = 1) \tag{2.4}$$

$$= \frac{h}{2998\,\mathrm{Mpc}} \qquad (\text{assuming } c = 1)\ . \tag{2.5}$$

In his seminal paper, Hubble estimated $h \sim 5$. The most accurate local measurements of h to date employ Cepheid variables and Type Ia supernovae in low-redshift galaxies, and read

$$h = 0.738 \pm 0.024 \qquad (\text{Riess et al. [69]})\ , \tag{2.6}$$

$$h = 0.743 \pm 0.021 \qquad (\text{Freedman et al. [31]})\ , \tag{2.7}$$

at 68 % confidence level. The Planck CMB satellite obtained a more precise value [67], but it is an indirect estimate as it assumes a cosmological (ΛCDM) model:

$$h = 0.6780 \pm 0.0077 \qquad (\text{Planck} + \text{WP} + \text{highL} + \text{BAO})\ , \tag{2.8}$$

at 68 % confidence level. There is a mild tension between the two measurements, which could be explained by some unknown source of systematic error in the local measurement or by the fact that the ΛCDM model assumed in Planck's data analysis is incorrect [67, 81].

On small scales the cosmological principle fails because, over time, gravitational instability creates bound structures such as stars, galaxies and clusters of galaxies. Hence, we expect galaxies to have their own motions decoupled from the Hubble expansion, which are called *peculiar velocities*. An example of peculiar velocity is the circular motion of the galaxies of a cluster around the common centre of mass. In most cases, the magnitude of the peculiar velocities does not exceed 10^3 km/s;

(Footnote 4 continued)
by Arthur Eddington and Willem de Sitter. An account by the American Institute of Physics of the fascinating story behind the discovery of the expansion of the Universe can be found at the following URL: http://www.aip.org/history/cosmology/ideas/expanding.htm.

using the measured values for H_0, we expect peculiar velocities to be negligible with respect to the Hubble flow for objects distant more than roughly 100 Mpc. It is reassuring that such a value is consistent with the homogeneity scale discussed in Sect. 2.2.

2.3.1 The Metric

The dynamics of the expanding Universe are better understood in terms of observers who are at rest with the Hubble expansion, the so-called *comoving observers*. Comoving observers perceive the Universe as isotropic and see objects receding from them according to Hubble's law. In this section, we shall employ *comoving coordinates* defined as the coordinate system where all comoving observers have constant spatial coordinates, i.e. are static. Any motion in comoving coordinates has the Hubble part subtracted so that the only velocities are the peculiar ones.

In differential geometry the distance ds between two infinitesimally nearby space-time points (x^0, x^1, x^2, x^3) and $(x^0 + dx^0, x^1 + dx^1, x^2 + dx^2, x^3 + dx^3)$ is called the line element and is defined as

$$ds^2 \;=\; g_{\mu\nu}\,(x)\; dx^\mu dx^\nu \;\;\text{for}\;\; \mu, \nu = 0, 1, 2, 3\;.$$

Here $g_{\mu\nu}(x)$ is the metric, a (0,2) tensor which determines how distances are computed in the considered space-time manifold. We shall adopt comoving coordinates and set $x^0 = c\,t$ where t is the cosmic time.

The metric that describes a homogeneous and isotropic expanding space-time is called the Friedmann-Lemaître-Robertson-Walker (*FLRW*) metric [32, 46, 70, 82]. In comoving coordinates, it is given by

$$ds^2 \;=\; -(c\,dt)^2 \;+\; a(t)^2\,\gamma_{ij}\,dx^i\,dx^j\;. \tag{2.9}$$

The *cosmic time* t, introduced in Sect. 2.2, is defined so that the Universe has the same density everywhere at each moment in time. The *scale factor* $a(t)$ parametrises the uniform expansion of the Universe. We express the spatial part of ds^2 so that, in comoving and spherical coordinates (ρ, θ, ϕ), it reads

$$\gamma_{ij}\,dx^i\,dx^j \;=\; d\rho^2 \;+\; S_k(\rho)^2\left(d\theta^2 + \sin^2\theta\,d\phi^2\right)\;. \tag{2.10}$$

With this choice, the quantity $d\chi^2 \equiv \gamma_{ij}\,dx^i\,dx^j$ has the meaning of a *comoving distance* or *coordinate distance*. The function $S_k(\rho)$ depends on the *spatial curvature* of the Universe, which in these models is uniform and is given by k/a^2. Even before discussing its form, it should be noted that for radial trajectories ($d\phi = d\theta = 0$) the comoving distance coincides with the radial comoving coordinate.

We distinguish three different geometries for the Universe based on the value of the curvature constant k:

$$S_k(\rho) = \begin{cases} \rho & \text{flat geometry} \quad (k=0) \\ \sin(\rho) & \text{spherical geometry} \quad (k=+1) \\ \sinh(\rho) & \text{hyperbolic geometry} \quad (k=-1)\ . \end{cases} \tag{2.11}$$

For $k = 0$, the comoving distance is just the usual Euclidean distance: $d\chi^2 = \delta_{ij}\, x^i x^j$. The value of the curvature constant k is a free parameter in the *FLRW* models and, as the Hubble constant, has to be determined by experiment. Recent results from the WMAP [39] and Planck [67] CMB satellites constrain the spatial curvature to be negligible, thus suggesting that we live in a Universe with a flat geometry. We shall assume $k = 0$ for the rest of this work. This allows us to choose coordinates where ρ and χ are lengths (measured in Mpc) and the scale factor is a dimensionless quantity such that $a(t_0) = 1$ [24].

Now that we have introduced the concept of scale factor, Hubble's law follows easily. Given an observer at the origin of a spherical coordinate system, we define the physical coordinates of an object as $\boldsymbol{r} = a(t)\,\boldsymbol{x}$, where $\boldsymbol{x} = (x^1, x^2, x^3)$ are its comoving coordinates. The distance $r = a(t)\,\chi$ along a radial path is the *physical distance* and can be thought as the distance that would be measured by stretching a tape measure in a uniformly curved surface [36]. There are two contributions to the velocity $d\boldsymbol{r}/dt$:

$$\frac{d\boldsymbol{r}}{dt} = \frac{1}{a}\frac{da}{dt}\boldsymbol{r} + a\,\frac{d\boldsymbol{x}}{dt}\ . \tag{2.12}$$

We project along the radial direction $\hat{\boldsymbol{r}}$ in order to obtain an expression for the radial velocity $v = d\boldsymbol{r}/dt \cdot \hat{\boldsymbol{r}}$:

$$v = \frac{1}{a}\frac{da}{dt}r + a\,\frac{d\boldsymbol{x}}{dt}\cdot\hat{\boldsymbol{r}}\ . \tag{2.13}$$

The term $a\,d\boldsymbol{x}/dt \cdot \hat{\boldsymbol{r}}$ is the *peculiar velocity* of the object. For a comoving object ($d\boldsymbol{x}/dt = 0$) we obtain the so-called *velocity-distance law*:

$$v = \frac{1}{a}\frac{da}{dt}r\ . \tag{2.14}$$

The above equation has the same form of Hubble's law in Eq. 2.1. From a direct comparison, we see that the Hubble constant H_0 is just the present-day value of the *Hubble parameter* defined as

$$H \equiv \frac{1}{a}\frac{da}{dt}\ . \tag{2.15}$$

Conformal time The *FLRW* metric can be conveniently expressed using the *conformal time* defined as $d\tau = dt/a$:

$$ds^2 = a(\tau)^2 \left\{ -(c\,d\tau)^2 + \gamma_{ij}\,dx^i\,dx^j \right\} = a(\tau)^2\,\eta_{\mu\nu}\,dx^\mu\,dx^\nu\,, \qquad (2.16)$$

where $\eta_{\mu\nu}$ is the Minkowski metric of special relativity and we have assumed flat space ($k = 0$). In the following chapters we shall use τ instead of t as the evolution variable for the cosmological perturbations, and assume units where $c = 1$. It should be noted that, for a radial trajectory, the conformal time is equal to the comoving distance divided by c.

2.3.2 Light in an Expanding Universe

The cosmological data that we extract from the Universe (temperature and polarisation maps, galaxy surveys, lensing maps, etc.) rely on the observation of light, with the exceptions of neutrinos and, possibly, gravitational radiation. It is therefore crucial to understand how light is affected by the expansion of the Universe.

2.3.2.1 Expansion Redshift

All physical lengths are stretched by the expansion of the Universe; the wavelength of a light wave makes no exception. Light emitted by a comoving source at time t with wavelength λ will be seen by a comoving observer today with a wavelength λ_0 given by

$$\frac{\lambda_0}{\lambda} = \frac{a(t_0)}{a(t)}\,.$$

As it travels through the expanding Universe, the light emitted from distant objects experiences an *expansion redshift*: its spectrum is uniformly shifted to larger wavelength and lower energies by an amount depending solely on the time of emission, regardless of whether the light consists of radio waves or gamma rays.

By adopting the same convention as in spectroscopy, where the fractional wavelength shift $(\lambda_0 - \lambda)/\lambda$ is denoted by the letter z, we write the *expansion-redshift law*

$$1 + z(t) = \frac{a(t_0)}{a(t)}\,. \qquad (2.17)$$

If we assume that the laws governing the emission and absorption of light do not change through cosmic evolution, the expansion redshift of a cosmological source can be inferred from its electromagnetic spectrum. Thanks to spectroscopic galaxy

surveys such as 2dF [18], SDSS-II [87], WiggleZ [23] and BOSS [20], we have now measured the optical spectra of millions of galaxies and thus determined their redshift.

In an expanding Universe, the sources with the highest redshift are the ones farthest away from us. Hence, high-redshift objects have to be more luminous than low-redshift ones for us to be able to see them. The highest-redshift galaxy that has been spectroscopically confirmed to date has $z = 7.51$ [29],[5] and a candidate galaxy with $z = 11.9$ [27] has been recently reported. In a ΛCDM Universe, the light from these galaxies was emitted about 13 billion years ago and their distance is now growing at a rate of many times the speed of light.

In the following, we will sometimes use the redshift as a time variable to parametrize the evolution of the Universe. This is correct since z is a monotonically decreasing function of a which in turn, in an expanding Universe, is a monotonically increasing function of cosmic time. Note also that from Eq. 2.17 it follows that today ($a(t_0) = 1$) the redshift vanishes: $z(t_0) = 0$.

2.3.2.2 Other Redshifts

The expansion redshift should not be confused with the Doppler effect. The Doppler effect produces a shift in the observed wavelength of photons because of the relative motion between source and observer. The recession velocity does not give rise to a Doppler shift because it does not describe the motion of objects in space, but the rate at which distances grow in the expanding Universe. Incidentally, this is why recession velocities can be larger than the speed of light. What gives rise to the expansion redshift is the wavelength of photons getting stretched during their trajectory through expanding space. On the other hand, Doppler redshift is generated by the peculiar velocities of the galaxies, which cannot exceed the speed of light.

A third type of redshift, the gravitational redshift, arises from the fact that the photons frequencies change as they travel through an inhomogeneous gravitational field. For example, we expect the light from a cluster of galaxies to be gravitationally redshifted, as the gravitational field at the centre of the cluster is different from that on the surface of Earth.

Expansion redshift, Doppler redshift and gravitational redshift coexist in the spectrum of galaxies and, in general, of all astrophysical sources. When determining the expansion redshift of an object, the non-cosmological Doppler and gravitational redshifts must be subtracted or accounted for in the error budget. The gravitational redshift is usually not too much of a concern as it shifts the spectrum by just $z \sim 10^{-3}$ [36]. However, in the local Universe, say for $z < 0.01$, the peculiar velocities give rise to a Doppler redshift of the same order of the expansion one. This is a manifestation of the breakdown of the cosmological principle on small scales due to

[5] Note that a galaxy with a spectroscopic redshift of $z = 8.6$ had been previously reported in Ref. [44], but it was later found to be a spurious signal in Ref. [12].

gravitational instability. For more distant objects, peculiar velocities become negligible with respect to recession velocities and one can trust the measured redshift to be due to the expansion of the Universe.

2.3.3 Comoving Distance

In Sect. 2.3.1 we have introduced the concept of comoving distance χ as the dimensionless distance between two spatial points on the comoving grid. The great advantage of χ is that it is constant in time, since its expression only involves comoving coordinates. On the other hand, the physical distance, given by $r = a(t)\chi$, is the tape-measure distance on a grid which is not comoving with the expansion, and hence increases with time.

But how are these theoretical distances related to the measured redshift of an object? Since redshift is intrinsically related to light propagation, we need to study the trajectory of photons from a source to us. This is described by the null geodesics ($ds^2 = 0$) along a radial path ($d\phi = d\theta = 0$),[6] which in the case of the *FLRW* metric in Eq. 2.9 yields

$$d\chi = \frac{c}{a}\, dt \,. \tag{2.18}$$

This result is intuitive: the actual speed of a photon does not vary, but its speed with respect to expanding coordinates is larger when the Universe is small ($a < 1$). A photon that was emitted at a time $t_{\rm ems}$ and observed at $t_{\rm obs}$ will have travelled a comoving distance of

$$\chi\,(t_{\rm ems}, t_{\rm obs}) = \int_{t_{\rm ems}}^{t_{\rm obs}} \frac{c}{a(t)}\, dt \,. \tag{2.19}$$

Any comoving distance is by construction independent of time. If another photon is emitted soon after the first one (say, at time $t_1 + dt_1$), it is obviously observed after the first one (say, at time $t_2 + dt_2$), but the comoving distance covered is the same. In formulae, $\chi\,(t_1, t_2) = \chi\,(t_1 + dt_1, t_2 + dt_2)$. Inserting this identity in Eq. 2.19 yields $dt_1/a(t_1) = dt_2/a(t_2)$: the quantity $dt/a(t)$ is conserved along the light cone. This is a formal demonstration of the fact that all time intervals get stretched while propagating through an expanding Universe. Since $d\lambda = cdt$, this is true also for all wavelengths.

Using the expansion-redshift law, $1+z = a_0/a$ and the definition of the expansion rate, $aH = da/dt$, the comoving distance can be related to the redshift by

[6] It should be noted that, given the choice of the spatial metric in Eq. 2.10, the comoving distance for a radial path is just the radial comoving coordinate.

$$d\chi \;=\; -\frac{c}{a_0\, H(z)}\, dz\;, \tag{2.20}$$

where $a_0 \equiv a(t_0)$. Thus, the comoving distance travelled by a photon emitted at a redshift z and received today ($z = 0$) is given by

$$\chi(z) \;=\; \frac{c}{a_0}\int_0^z \frac{dz}{H(z)} \;=\; \frac{c}{a_0\, H_0}\int_0^z \frac{dz}{E(z)}\;, \tag{2.21}$$

where we have defined the dimensionless parameter $E(z) \equiv H(z)/H_0$ [6]. We shall refer to the above formula as the *distance-redshift law*; it is important because it relates the geometry of the Universe (χ and H) to the measured redshift. By using the velocity-distance relation $v = H_0\, r$ and the identity $r(t, t_0) = a_0\, \chi(t, t_0)$, we obtain the *velocity-redshift law*

$$\frac{v}{c} \;=\; \int_0^z \frac{dz}{E(z)}\;, \tag{2.22}$$

which is key to convert a redshift to the recession velocity at the time of emission.

The distance-redshift and velocity-redshift laws tell us that, in order to infer the distances and velocities of an object, we first need to know the expansion history of the Universe $H(z)$ all the way to when the light was emitted. The reason is that our cosmological observations are limited to the region of space-time included in our past light cone. We, as observers, do not have access to a the world map but only to a single world picture taken now and here [36]. The farthest sources in our world picture emitted their light at a time where the expansion rate was significantly different from the current value, H_0. Furthermore, the emitted light travelled for a long time in an expanding Universe. Hence, the measured redshift is related to the distance covered by the light by the expansion history between emission time and observation time.

If the object is very close, however, the integral $\int_0^z dz/E(z)$ can be Taylor expanded around $z = 0$ [6]:

$$\int_0^z \frac{dz}{E(z)} \;\simeq\; z \;-\; \frac{E'(0)}{2}z^2 \;+\; \frac{1}{6}\Big[2E'(0)^2 \;-\; E''(0)\Big]\, z^3 \;+\; \mathcal{O}(z^4)\;, \tag{2.23}$$

where the prime represents a derivative with respect to z. By keeping only the first term in the expansion, the distance-redshift and velocity-redshift laws become respectively

$$c\, z \;=\; H_0\, r \tag{2.24}$$

and

$$v \;=\; c\, z\;. \tag{2.25}$$

In his famous 1929 paper, Hubble interpreted his velocity measurements as peculiar velocities rather than recession velocities. He used the Fizeau-Doppler formula to convert redshifts in velocities, which happens to coincide with the $z \to 0$ limit of the velocity-redshift law. For this reason, some authors prefer to refer to $cz = H_0 r$ as the Hubble's law (rather than $v = H_0 r$) in order to keep clear the distinction between the Doppler redshift and velocity redshift [36].

2.3.4 The Hubble Time

The *Hubble time* t_H is defined as the inverse of the Hubble parameter. The current value of the Hubble time is easily obtained from the definition of H_0 in Eq. 2.2:

$$t_{H_0} \equiv \frac{1}{H_0} = 9.77\, h^{-1}\,\mathrm{Gyr}\ .$$

Given constant expansion, i.e. $d^2a/dt^2 = 0$, the Hubble time is the time needed by the Universe to double in size. Equivalently, the solution to:

$$a(t_1) + \frac{da}{dt}\,\Delta t = a(t_2)\ , \tag{2.26}$$

for $a(t_2) = 2a(t_1)$ is $\Delta t = H^{-1}(t_1)$. If the expansion had been constant after the Big Bang, the Hubble time would be the age of the Universe; to see it, substitute $a(t_1) = 0$ and $a(t_2) = a$ in the above equation.

In a more realistic model where the expansion rate varies, the Hubble time does not correspond anymore to the age of the Universe. It rather sets the time-scale for the expansion of the Universe: in a time comparable to H^{-1} the expansion parameter increases noticeably. In the currently accepted accelerating ΛCDM model, t_{H_0} is still a good proxy for the current age of the Universe. Using Planck cosmological parameters [67], one finds $t_0 = 13.817 \pm 0.048\,\mathrm{Gyr}$ against $t_{H_0} \simeq 14.6\,\mathrm{Gyr}$.

2.3.5 The Hubble Radius

The *Hubble radius* L_H is defined as the physical distance travelled by light in a Hubble time. From Eq. 2.2, its current value is given by

$$L_{H_0} \equiv \frac{c}{H_0} = 2998\,\mathrm{h}^{-1}\,\mathrm{Mpc}\ . \tag{2.27}$$

By virtue of the velocity-distance law ($v = Hr$), objects farther than a Hubble radius recede faster than light.[7] Therefore, given a constant expansion, an object located at the centre of a sphere whose radius is equal to the Hubble radius will never be able to interact with objects outside the sphere; a super-luminar motion is necessary for the contrary to be true. In these conditions, the Hubble radius is the maximum extension of the future light cone of any event in the Universe.

However, if the expansion of the Universe slows down, the Hubble sphere swells and an increasing number of regions in the Universe will eventually enter in causal contact. The time-scale needed for this to happen is the Hubble time. On the other hand, if the Universe experiences an accelerated expansion, any object located inside the Hubble sphere now will be out of it after a long enough time; as a result an increasing number of causally disconnected regions will be created. In an accelerating Universe light cannot keep up with the expansion.

Because of this causal interpretation, the Hubble radius is often referred to as *horizon*. Being defined as

$$\frac{c}{H(t)} ,$$

the horizon is a physical distance, not a comoving one. Its comoving counterpart is obtained by dividing it by the expansion parameter:

$$\frac{c}{a(t)\, H(t)} .$$

The above quantity, called the *comoving horizon*, is not to be confused with the *particle horizon*, which we define below and represents the maximum distance a particle could have travelled since the Big Bang until a certain time t.

2.3.5.1 Particle Horizon and Causality

The distance travelled by a photon from the Big Bang up to a certain time t is known as the *particle horizon*. Its expression in comoving coordinates is obtained from Eq. 2.19 by setting $t_{\rm ems} = 0$ and $t_{\rm obs} = t$:

$$\chi(t) \equiv \int_0^t c\, \frac{dt}{a(t)} .$$

Since the speed of light is the limit velocity, the particle horizon represents the maximum comoving distance any particle could have travelled up to time t. Note that the particle horizon is proportional to the conformal time τ appearing in Eq. 2.16:

[7] Note that this behaviour does not invalidate special relativity since expansion is uniform everywhere in the Universe and therefore no exchange of information is possible as a result of the super-luminar velocity.

$$\chi(t) \;=\; c\,\tau(t)\;. \tag{2.28}$$

In the following we shall use the conformal time and the comoving particle horizon interchangeably.

At any moment t in the evolution of the Universe, the particle horizon $\chi(t)$ is the maximum extension of the past light cone for all events in the Universe. In particular, for an observer on Earth, the present-day particle horizon sets the size of the observable Universe. Its value depends on the cosmological model adopted; for a ΛCDM model, it roughly amounts to $\chi(t_0) \simeq 14{,}000\,\mathrm{Mpc}$. For the same model, $c\,t_0 \simeq 4{,}000\,\mathrm{Mpc}$. There is a subtle difference between the particle horizon $\chi(t)$ and the Hubble horizon $c/(aH)$: the former is a measure of the past light cone of an event given the previous expansion history, while the latter sets the extent of its future light cone based on the instantaneous value of H.

2.4 The Background Evolution

In order to derive the time evolution of the scale parameter $a(t)$ we need to relate the metric with the energy content of the Universe. This is achieved via the *Einstein equation*:

$$R_{\mu\nu} \;-\; \frac{1}{2}\,g_{\mu\nu}\,R \;=\; 8\,\pi\,G\;T_{\mu\nu}\;, \tag{2.29}$$

where we have set $c = 1$ and

- $R_{\mu\nu}$ is the Ricci tensor, defined as the self-contraction of the Riemann tensor. It can be expressed in terms of the *Christoffel symbols* or *affine connection*,

$$\Gamma^{\mu}{}_{\alpha\beta} \;=\; \frac{g^{\mu\nu}}{2}\left[\;\frac{\partial g_{\alpha\nu}}{\partial x^{\beta}} \;+\; \frac{\partial g_{\beta\nu}}{\partial x^{\alpha}} \;-\; \frac{\partial g_{\alpha\beta}}{\partial x^{\nu}}\;\right] \tag{2.30}$$

  as

$$R_{\mu\nu} \;=\; \frac{\partial \Gamma^{\alpha}{}_{\mu\nu}}{\partial x^{\alpha}} \;-\; \frac{\partial \Gamma^{\alpha}{}_{\mu\alpha}}{\partial x^{\nu}} \;+\; \Gamma^{\alpha}{}_{\beta\alpha}\,\Gamma^{\beta}{}_{\mu\nu} \;-\; \Gamma^{\alpha}{}_{\beta\nu}\,\Gamma^{\beta}{}_{\mu\alpha}\;. \tag{2.31}$$

- $R \;=\; g_{\mu\nu}\,R^{\mu\nu}$ is the Ricci scalar.
- $T_{\mu\nu}$ is the total energy-momentum tensor, source of the gravitational field.
- G is Newton's gravitational constant.

Inserting the metric for an *FLRW* Universe in comoving coordinates (Eq. 2.9), we find that for an isotropic Universe the only non-zero components of the connection, Ricci tensor and Ricci scalar are, respectively,

$$\Gamma^0{}_{ij} = \delta_{ij}\, a'\, a \qquad \text{and} \qquad \Gamma^i{}_{0j} = \Gamma^i{}_{j0} = \delta_{ij}\, \frac{a'}{a}\,, \tag{2.32}$$

$$R_{00} = -3\, \frac{a''}{a} \qquad \text{and} \qquad R_{ij} = \delta_{ij} \left(2\, a'^2 + a\, a''\right)\,, \tag{2.33}$$

$$R = 6 \left[\frac{a''}{a} + \left(\frac{a'}{a}\right)^2 \right]\,, \tag{2.34}$$

where the primes denote differentiation with respect to cosmic time, $a' = da/dt$. The left hand side of the Einstein equation is called the *Einstein tensor* $G_{\mu\nu}$ and can be determined using the above relations:

$$G_{00} = 3 \left(\frac{a'}{a}\right)^2\,, \quad G_{ij} = -\delta_{ij} \left(a'^2 + 2\, a\, a''\right) \quad G_{i0} = G_{0i} = 0\,. \tag{2.35}$$

The total energy-momentum tensor is given by the sum of the energy-momentum tensors of the species in the Universe, that is,

$$T_{\mu\nu} = \sum_a T_{a,\mu\nu}\,, \tag{2.36}$$

where $a = \gamma, b, \nu, c, \Lambda$ for photons, baryons, neutrinos, cold dark matter and dark energy, respectively. The fact that the spatial Einstein tensor is diagonal is a direct consequence of the isotropy of the *FLRW* metric. The energy-momentum is forced to be diagonal too, meaning that the cosmological fluids cannot have peculiar velocities or anisotropic stresses. Therefore, in the simple *FLRW* model a fluid is characterised only by its energy density $\rho(t)$ and its pressure $P(t)$.

We shall assume that the fluids that compose the Universe are *barotropic*, that is, their pressure is given as an explicit function of their energy density. The relation between P and ρ is called the *equation of state* of the fluid; we parametrise it via the barotropic parameter w as

$$P = w(\rho)\, \rho\,. \tag{2.37}$$

The energy-momentum tensor of the fluid 'a' is thus expressed as

$$T_{a,00} = \rho_a\,, \qquad\qquad T_{a,ij} = \delta_{ij}\, w_a(\rho)\, \rho_a\,. \tag{2.38}$$

As we shall soon see, knowing the equation of state $w(\rho)$ of the various species is needed to derive the expansion history of the Universe. Relativistic species (R), such as the photons, the neutrinos and the massive species while still relativistic, have a constant equation of state: $w_R = \frac{1}{3}$. Non-relativistic species (M), such as the baryons and cold dark matter after decoupling, instead, have no pressure: $w_{\rm M} = 0$. Note that,

already in a simple mixture of matter and radiation, w ceases to be constant. In this work we treat dark energy as a cosmological constant, which is equivalent to a negative pressure fluid with constant equation of state: $w_\Lambda = -1$.

2.4.1 Friedmann Equation

The time-time component of the Einstein equations is called the *Friedmann equation*,

$$H^2 \;=\; \frac{8\,\pi\,G}{3}\,\rho \;-\; \frac{k}{a^2}\;, \tag{2.39}$$

where $H = a'/a$ is the Hubble parameter and $\rho = \sum \rho_a$ is the total energy density of the Universe. We have included the curvature contribution, k, to highlight the fact that in a flat universe ($k = 0$) the total density always equals the *critical density* $\rho_{\rm crit}$, defined as

$$\rho_{\rm crit} \;\equiv\; \frac{3\,H^2}{8\,\pi\,G}\;.$$

The critical density depends on time; its present-day value can be easily computed in terms of the Hubble constant:

$$\rho_{\rm crit}(t_0) \;=\; 1.878\;{\rm h}^2 \;\times\; 10^{-26}\;\frac{\rm kg}{\rm m^3} \tag{2.40}$$

$$\;=\; 2.775\;{\rm h}^{-1} \;\times\; 10^{11}\;\frac{\rm M_\odot}{\left(h^{-1}\,{\rm Mpc}\right)^3} \tag{2.41}$$

$$\;=\; 10.54\;{\rm h}^2\,\frac{\rm GeV}{\rm m^3} \qquad\qquad (\text{assuming } c = 1)\;. \tag{2.42}$$

This is an astonishingly small number: with a density of $1.27\,{\rm kg/m^3}$, air is around 10^{26} times denser than the critical density. However, since 10^{11}–10^{12} solar masses is close to the mass of a typical galaxy and 1 Mpc is the order of magnitude of the typical galaxy separation, the Universe cannot be too distant from the critical density.

The density of the species normalised to the critical density of the Universe is called the *density parameter*:

$$\Omega_a(t) \;\equiv\; \frac{\rho_a(t)}{\rho_{\rm crit}(t)}\;. \tag{2.43}$$

Using the information on the equations of state of the various species (Sect. 2.4.3), the Friedmann equation can be recast in terms of the present-day value of the density parameters, $\Omega_{a0} \equiv \Omega_a(t_0)$, as

$$H^2 \;=\; H_0^2 \left[\frac{\Omega_{\rm M0}}{a^3} \;+\; \frac{\Omega_{\rm R0}}{a^4} \;+\; \frac{\Omega_{k0}}{a^2} \;+\; \Omega_{\Lambda 0} \right] , \tag{2.44}$$

where $H_0 \equiv H(t_0)$ and

$$\Omega_{\rm M0} \;=\; \frac{\rho_{\rm M}(t_0)}{\rho_{\rm crit}(t_0)} , \quad \Omega_{\rm R0} \;=\; \frac{\rho_{\rm R}(t_0)}{\rho_{\rm crit}(t_0)} , \quad \Omega_{k0} \;=\; -\frac{k}{a_0^2\, H_0^2} , \quad \Omega_{\Lambda 0} \;=\; \frac{\Lambda}{3\, H_0^2} . \tag{2.45}$$

(In this thesis, cosmological quantities indexed by a '0' are evaluated today, $X_0 \equiv X(t_0)$).

2.4.2 Acceleration Equation

In an *FLRW* Universe, the spatial components of the Einstein equation reduce to a single expression, the *acceleration equation*:

$$\frac{a''}{a} \;=\; -\frac{4\,\pi\, G}{3} \;(\rho \;+\; 3\, P) \;, \tag{2.46}$$

where $P \;=\; \sum P_a$ is the combined pressure of all the species. The acceleration equation holds also in a curved Universe, where $k \neq 0$.

The pressure and the density appear in the acceleration equation on equal grounds: they both contribute to increasing the gravitational attraction and thus decelerate the cosmic expansion. This might seem counter intuitive, as we are used to thinking of pressure as something that powers expansive processes such as explosions. This is indeed true if a force is supplied by means of a gradient in the pressure field; however, in a homogeneous Universe, P is the same everywhere and no pressure forces are possible.

2.4.3 Continuity Equation

The evolution of the matter species is determined by the conservation of the energy and momentum,

$$T^{\mu}{}_{\nu;\mu} \;=\; \partial_\mu T^{\mu}{}_{\nu} \;+\; \Gamma^{\mu}{}_{\alpha\mu} T^{\alpha}{}_{\nu} \;-\; \Gamma^{\alpha}{}_{\nu\mu} T^{\mu}{}_{\alpha} \;=\; 0 \,. \tag{2.47}$$

Due to isotropy, the only meaningful equation is $\nu = 0$, the *continuity equation*:

$$\rho' \;+\; 3\, H \;(\rho \;+\; P) \;=\; 0 \,, \tag{2.48}$$

which, in terms of the barotropic parameter, reads

$$\rho' \, + \, 3 \, H \, \rho \, (w \, + \, 1) \, = \, 0 \, . \tag{2.49}$$

The continuity equation applies separately to each species as, for the epochs of interest, their particle number is conserved and their energy exchange is negligible. Then, for a fluid 'a' with a constant equation of state, $P \, = \, w \rho$, the continuity equation can be solved to yield

$$\rho_a \, \propto \, a^{-3\,(1\,+\,w_a)} \, . \tag{2.50}$$

For radiation ($w \, = \, 1/3$), cold matter ($w \, = \, 0$) and the cosmological constant ($w \, = \, -1$), the density is thus given by

$$\rho_{\rm R} \, \propto \, a^{-4} \, , \qquad \rho_{\rm M} \, \propto \, a^{-3} \, , \qquad \rho_{\Lambda} \, = \, \text{constant} \, . \tag{2.51}$$

In the more general case of a time-dependent equation of state, $w \, = \, w(a)$, one has to solve the following integral:

$$\rho \, \propto \, \exp \left(-3 \int_0^a \frac{{\rm d}\tilde{a}}{\tilde{a}} \, \left[1 \, + \, w(\tilde{a}) \right] \right) \, . \tag{2.52}$$

2.4.4 Expansion History

The expansion history of a universe filled by a single species with constant equation of state can be inferred analytically. This is achieved by inserting the general equation of state (Eq. 2.50) into the Friedmann equation (Eq. 2.39) and solving for $a(t)$. If the curvature k is neglected, we have that [24]

$$\begin{array}{lll}
a \, \propto \, t^{2/(3\,(1+w))} \, \propto \, \tau^{2/(1+3w)} \, , & H \, \propto \, t^{-1} \, \propto \, a^{-3(1+w)/2} \, , & w \, = \, \text{constant} \, \neq \, -1 \, , \\
a \, \propto \, t^{2/3} \, \propto \, \tau^2 \, , & H \, \propto \, t^{-1} \, \propto \, a^{-3/2} \, , & w \, = \, 0 \quad \text{(cold matter)} \, , \\
a \, \propto \, t^{1/2} \, \propto \, \tau \, , & H \, \propto \, t^{-1} \, \propto \, a^{-2} \, , & w \, = \, 1/3 \quad \text{(radiation)} \, , \\
a \, \propto \, e^{H \, t} \, \propto \, 1/|\tau| \, , & H \, = \, \text{constant} \, , & w \, = \, -1 \quad \text{(cosmol. constant)} \, .
\end{array} \tag{2.53}$$

Recall that t is the cosmic time and τ is the conformal time, $d\tau = dt/a$.

In the general case of a mixture of fluids, one has to rely on the full Friedmann equation (Eq. 2.44):

$$\frac{1}{a} \frac{da}{dt} \, = \, H_0 \, \sqrt{\frac{\Omega_{\rm M0}}{a^3} \, + \, \frac{\Omega_{\rm R0}}{a^4} \, + \, \frac{\Omega_{k0}}{a^2} \, + \, \Omega_{\Lambda 0}} \, , \tag{2.54}$$

which yields a time integral that is easily solved for $a(t)$ once the cosmological parameters are specified. These have been measured to high accuracy. For the Hubble

constant, $H_0 = 100\,h$ km/s/Mpc, and the density parameter of matter, $\Omega_{\rm M} = \Omega_b + \Omega_c$, we adopt the best fit values obtained by the Planck experiment [67],

$$h = 0.6780 \pm 0.0077\,, \quad \Omega_{b0}\,h^2 = 0.02214 \pm 0.00024\,, \quad \Omega_{c0}\,h^2 = 0.1187 \pm 0.0017\,, \tag{2.55}$$

at 68 % confidence level. The density parameter of the photon fluid is determined by the value of the CMB temperature [30],

$$T_0 = 2.725 \pm 0.001\,\text{K} \qquad \text{at 95 \% confidence level}\,, \tag{2.56}$$

which, for a blackbody spectrum, yields

$$\Omega_{\gamma 0}\,h^2 = 2.49 \times 10^{-5} \qquad \text{and} \qquad \Omega_{\nu 0}\,h^2 = 1.69 \times 10^{-5}\,, \tag{2.57}$$

where we have used the fact that the massless neutrino density is roughly equal to $0.68\,\Omega_\gamma$ because they are fermions rather than bosons and are at a lower temperature. Finally, we assume a flat Universe ($\Omega_k = 0$) so that the density of dark energy can be determined as

$$\Omega_{\Lambda 0} = 1 - \Omega_{\rm R0} - \Omega_{\rm M0} = 0.694\,. \tag{2.58}$$

In Fig. 2.1 we show the evolution of the scale factor obtained for the above parameters. Depending on the species that is the most abundant, we identify three epochs in the cosmic history: the *radiation dominated era* ($a \propto \tau$), the *matter domination*

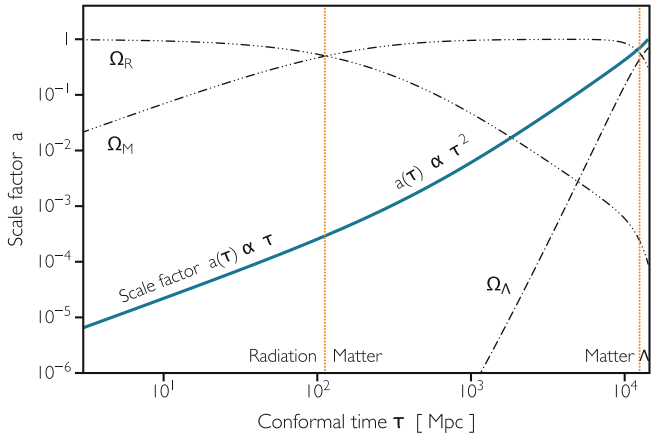

Fig. 2.1 Cosmic history of the Universe. The *blue curve* is the scale factor as a function of conformal time, obtained by solving the Friedmann equation in Eq. 2.54. Today corresponds to $a = 1$ and $\tau = 14{,}200$ Mpc. The three *black dot-dashed curves* are the density parameters of radiation ($\Omega_{\rm R}$), cold matter ($\Omega_{\rm M}$) and dark energy considered as a cosmological constant fluid (Ω_Λ). The intersections between the three Ω's naturally split the cosmic history in three epochs: the radiation domination era ($a \propto \tau$), the matter domination era ($a \propto \tau^2$) and the dark energy domination era ($a \propto 1/\tau$)

era ($a \propto \tau^2$) and the *dark-energy dominated era* ($a \propto 1/\tau$). The transitions between the three eras take place at

$$a_{\rm eq} \;=\; \frac{\Omega_{\rm R0}}{\Omega_{\rm M0}} \;=\; 2.96 \times 10^{-4} \qquad \text{and} \qquad a_\Lambda \;=\; \frac{\Omega_{\rm M0}}{\Omega_{\Lambda 0}} \;=\; 0.44\,, \tag{2.59}$$

which correspond, respectively, to $z_{\rm eq} = 3380$ and $z_\Lambda = 1.26$.

The Big Bang If we inspect the acceleration equation Eq. 2.46,

$$\frac{a''}{a} \;=\; -\frac{4\,\pi\,G}{3}\;\rho\;(3\,w\;+\;1)\;, \tag{2.60}$$

we see that in the early Universe when radiation dominates ($w = 1/3 > 0$), the second derivative of $a(t)$ is negative; that is, $a(t)$ is a concave curve. Thus, we expect the scale factor of the Universe to cross the $a = 0$ line in a finite amount of time; the moment when this happens is called the *Big Bang*.[8] The Big Bang represents a singularity in the coordinates (the spatial metric vanishes for $a = 0$), in the Ricci scalar (Eq. 2.34) and in the density ($\rho_{\rm R} \propto a^{-4}$).

2.5 The Cosmic Microwave Background

Soon after the Big Bang, the particle density is so high that the species interact at a rate much higher than the expansion rate, with all kinds of particle-antiparticle pairs being created and annihilated. As a result of these continuous collisions, particles of different species are in *thermal equilibrium*, i.e. they can be considered to be part of a single *cosmic plasma* with a common temperature and average kinetic energy.

Photons in thermal equilibrium obey a *blackbody spectrum*, which is characterised by a simple relation between the energy density ρ_γ and the ambient temperature T,

$$\rho_\gamma \;=\; \alpha\;T^4\;, \tag{2.61}$$

where the proportionality constant is the Stefen-Boltzmann constant times $4/c$, that is, $\alpha = \pi^2 k_{\rm B}^4/(\hbar^3 c^3)$. Since the energy density of radiation scales with a^{-4}, it follows that the temperature of the cosmic plasma scales as a^{-1}:

$$T \;=\; \frac{2.725\,{\rm K}}{a} \;=\; (z+1)\;2.35 \times 10^{-4}\,{\rm eV}\;, \tag{2.62}$$

where we have used the current CMB temperature as normalisation and, in the second equality, we have assumed units where the Boltzmann constant $k_{\rm B} = 11{,}605^{-1}\,{\rm eV/K}$

[8] The name was invented during a radio interview by Fred Hoyle, the main supporter of a steady state Universe, as a mockery of the idea of an expanding Universe. Refer to the following URL for the transcript: http://www.joh.cam.ac.uk/library/special_collections/hoyle/exhibition/radio/.

is equal to one. To give an idea of the scales involved, we can use the fact that $a \propto t^{1/2}$ in the radiation dominated era to write

$$T \simeq 1.5 \times 10^{10}\,\mathrm{K}\,\sqrt{\frac{1\mathrm{s}}{t}} \simeq 1.3\,\mathrm{MeV}\,\sqrt{\frac{1\mathrm{s}}{t}}\,, \tag{2.63}$$

Thus, one second after the Big Bang, the average photon has an energy of $\sim$1 MeV while, after 50,000 years, its energy has dropped to 1 eV.

In an expanding Universe, however, thermal equilibrium does not last forever. The particles of a given species interact with a rate proportional to their number density, which decays as a^{-3}. The expansion rate H, on the other hand, never decays faster than $a^{-3/2}$ (Eq. 2.53), meaning that, eventually, it will exceed the interaction rate. As a result, the thermal equilibrium cannot be maintained anymore and the particle species is said to have *decoupled* from the cosmic plasma. As we shall see in the next sections, the photons decouple at a redshift of $z \simeq 1100$, soon after matter-radiation equality. Then, why do we speak of "temperature of the photons", if they are not in thermal equilibrium? The answer is simple: the cosmic expansion preserves the blackbody spectrum of the photon fluid even when it is out of thermal equilibrium. Due to its E/T dependence, the distribution function is frozen as it redshifts into a similar distribution with a lower temperature proportional to $1/a$ (we will come back to this point in Sect. 4.3.1). Thus, after decoupling, the photon fluid possesses an effective temperature rather than a thermodynamical one.

The presence of this blackbody, isotropic background radiation of cosmic origin is a definite prediction of the Big Bang model. The first measurement that was directly linked [21] to the cosmic background radiation was made serendipitously in 1963 by Penzias and Wilson [65], who measured an isotropic excess temperature of around 3.5 K. Since then, many experiments were performed to measure the present-day CMB spectrum over different wavelengths. The most accurate measurement of the CMB spectrum was made by the FIRAS experiment, launched in 1989 on board of the NASA Cosmic Background Explorer (COBE). The spectrum measured by FIRAS [30, 54] is blackbody to high accuracy and is shown in Fig. 2.2. The blackbody form of the CMB spectrum has been confirmed by several other experiments for wavelengths outside the millimetre range, as shown in Fig. 2.3. The measured CMB temperature, $T_0 = 2.725 \pm 0.001$ K [30], implies that the average CMB photon has the following properties:

$$\text{frequency} \sim 160\,\mathrm{GHz}\,, \quad \text{wavelength} \sim 2\,\mathrm{mm}\,, \quad \text{energy} \sim 0.7\,\mathrm{meV}\,. \tag{2.64}$$

2.5.1 Compton Scattering

After the temperature of the cosmic plasma has dropped below the electron mass, $T \ll 511$ keV, the only process that maintains the photons in thermal equilibrium are the rapid collisions with the free electrons. In general, the scattering of a photon by

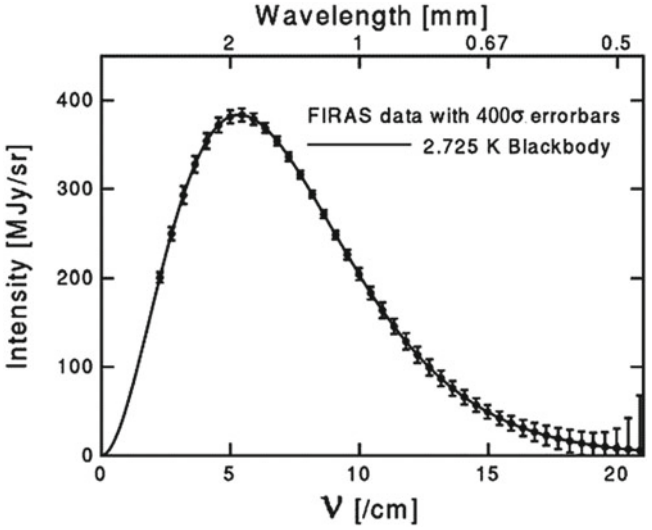

Fig. 2.2 The cosmic microwave background spectrum as measured by FIRAS. The *error bars* have been multiplied by 400 to make them visible; the *line* represents the best-fit blackbody spectrum at $T = 2.725\,\mathrm{K}$. *Source* Data from FIRAS [30], image courtesy of Edward L. Wright from the website http://www.astro.ucla.edu/~wright/cosmo_01.htm

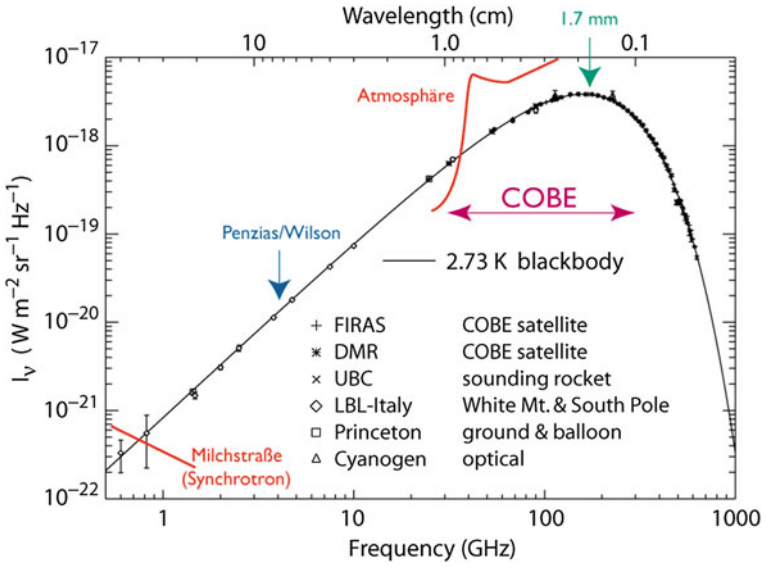

Fig. 2.3 The CMB blackbody spectrum as confirmed by measurements over a broad range of wavelengths. Credit: Fig. 19.1 of Ref. [61], reproduced with permission of Springer Publishing (http://pdg.lbl.gov/1998/contents_large_sports.html); coloured additions courtesy of Karl-Heinz Kampert (http://astro.uni-wuppertal.de/~kampert/Cosmology-WS0607.html)

a free charged particle is called *Compton scattering*. It is an inelastic process, as an incident photon deflected by an angle θ experiences a wavelength shift $\Delta\lambda \equiv \lambda' - \lambda$ of

$$\Delta\lambda \;=\; \lambda_c \;(1 \,-\, \cos\theta) \;, \tag{2.65}$$

where $\lambda_c \equiv h/(mc)$ is the Compton wavelength of the target particle, which is assumed to be at rest. In terms of the photon's energy ($E_\gamma = hc/\lambda$), the formula translates to

$$\frac{\Delta E_\gamma}{E'_\gamma} \;=\; (\cos\theta - 1)\,\frac{E_\gamma}{m\,c^2} \;, \tag{2.66}$$

which means that the fractional change in the photon's energy is negligible as long as its energy is much smaller than the target's mass. The condition definitely applies to our context, where we consider temperatures of the order of the eV and the target particles are electrons with $m_e c^2 = 511\,\text{keV}$.[9] In this limit, the process is elastic and is called *Thomson Scattering*.

The total cross-section for the Thomson scattering is given by [22]

$$\sigma_T \;=\; \frac{8\pi}{3}\,\alpha^2\,\lambda_c^2 \;=\; \frac{8\pi}{3}\left(\frac{\alpha\hbar}{mc}\right)^2 \tag{2.67}$$

$$\;=\; 6.652 \times 10^{-29}\text{m}^2 \tag{2.68}$$

$$\;=\; 4.328 \times 10^{-17}\text{eV}^{-2} \qquad (\text{assuming } h = c = 1)\;, \tag{2.69}$$

where $\alpha \simeq 1/137$ is the fine structure constant and in the last equalities we have used the electron mass $m_e c^2 = 511\,\text{keV}$. It is important to note that the cross section is inversely proportional to the squared mass of the target particle. Therefore, provided that protons and electrons have the same number density, photon-electron collisions ($m_e c^2 = 511\,\text{keV}$) are several million times more likely that photon-proton collisions ($m_p c^2 = 938\,\text{GeV}$). For this reason, we shall ignore the latter and focus on the former.

2.5.1.1 Interaction Rate and Optical Depth

Here we introduce the interaction rate $\dot{\kappa}$ and the optical depth κ that will be useful in the following chapters to derive and numerically solve the Boltzmann equation.

The cross-section σ associated with a scattering process is defined so that

$$dN \;=\; n\,\sigma\,dx \tag{2.70}$$

[9] Note that, in the context of the cosmological perturbations, even this tiny energy transfer has to be considered, as we shall see in Sect. 4.5.2.

is the average number of scatterings the incident particle undergoes when covering a distance of dx in a material with a density n of scattering targets. Since dN/dx is the average number of scatterings per unit of length, its inverse is the *mean free path*:

$$\lambda = \frac{1}{n\,\sigma}\,, \tag{2.71}$$

i.e. the average distance a particle covers between two consecutive scatterings. If the velocity dx/dt of the incident particle is known, then it is straightforward to obtain the *interaction rate* dN/dt, that is the average number of scatterings per unit of time. For a photon,

$$\frac{dN}{dt} = n\,\sigma\,c\,. \tag{2.72}$$

The inverse of the interaction rate is the average time elapsed between two consecutive scatterings; we shall call this quantity *mean free time*. For a photon it is given by:

$$t_\gamma = \frac{1}{n\,\sigma\,c}\,. \tag{2.73}$$

In the context of the cosmic microwave background, the *optical depth* or *optical depth*, κ, is the average number of Thomson scatterings a photon undergoes from the time t up to now,

$$\kappa(t) = \int_t^{t_0} dt'\,n_e\,\sigma_T\,c\,. \tag{2.74}$$

The optical depth is a monotonically decreasing function of time; its time derivative is just the interaction rate with a negative sign

$$\frac{d\kappa}{dt} = -n_e\,\sigma_T\,c\,. \tag{2.75}$$

In terms of conformal time, $d\tau = dt/a$, the interaction rate reads

$$\dot{\kappa} = \frac{d\kappa}{d\tau} = -a\,n_e\,\sigma_T\,c\,. \tag{2.76}$$

2.5.2 Recombination and Decoupling

The frequent Thomson scatterings between the photons and the electrons before recombination keep the two fluids in thermal equilibrium. Together with the protons,

which are tightly coupled with the electrons via Coulomb scattering, the three species form a unique fluid with a common temperature.

The photons are maintained in thermal equilibrium as long as their interaction rate with the electrons, $n_e \sigma_T c$, exceeds the cosmic expansion rate, H. If we assume that the electrons remain free throughout cosmic evolution, such decoupling happens only at a redshift of $z \sim 40$ [22]. The electrons, however, do not stay free as it is energetically favourable for them to combine with the free protons to form hydrogen atoms via the reaction

$$e^- + p \quad \longrightarrow \quad \mathrm{H} + \gamma\,(13.6\,\mathrm{eV})\ . \tag{2.77}$$

In the early Universe, the energy and the density of photons are so high that the hydrogen atoms thus formed are rapidly disrupted via the inverse reaction; thus, most of the electrons are free and the abundance of neutral hydrogen is very low. As the Universe expands and cools, however, more and more atoms are able to form and endure in a process that is called *recombination*.

During recombination, the number density of free electrons quickly drops and so does the rate of photon scatterings, $|d\kappa/dt| = n_e \sigma_T c$. When the interaction rate is surpassed by the expansion rate, the photon fluid goes out of equilibrium and decouples from the electron fluid. As a result, the photons can stream freely in a now transparent Universe. This process is called *decoupling*. As we shall see below, decoupling happens during recombination.

Recombination is a complicated process that involves non-equilibrium physics and is usually treated using the Boltzmann formalism. In principle, to obtain the ionisation history of the Universe requires solving a system with 300+ differential equations, one per energy level of the hydrogen atom [73]. In practice, however, one can model the hydrogen atom as having effectively three energy levels: ground state, first excited state and continuum [63] (see also Sect. 5.3.4). Numerical codes such as *RECFAST* [73] start from this 3-level approximation to compute the ionisation history of the Universe in less than a second with sub-percent accuracy over a wide range of redshifts. The code *HyRec* [4] implements an even more accurate numerical treatment of recombination where four energy levels are considered that is mathematically equivalent to the multi-level approach [3].

However, it is still possible to make general statements about recombination and decoupling without resorting to a numerical computation, and we shall do so in the following two subsections. One of the major simplifications that we shall adopt is to assume that all the protons are in hydrogen nuclei, thus ignoring the $\sim$25 % contribution in mass that is expected from the helium nuclei. Since about 1 proton out of every 8 is in a Helium nucleus, this results in an error of roughly 10 %.

2.5.2.1 Recombination

The quantity of interest is the *free electron fraction* or *ionisation fraction*,

$$x_e \equiv \frac{n_e}{n_e + n_H} , \tag{2.78}$$

where n_e, n_p and n_H are respectively the number densities of free electrons, free protons and neutral hydrogen atoms; note that, since the Universe is globally neutral, $n_e = n_p$. If we neglect the small number of electrons and protons in Helium nuclei, the denominator is equal to the number density of baryons: $n_e + n_H \simeq n_b$.

Before recombination begins, the reaction $e + p \longleftrightarrow \mathrm{H} + \gamma$ is in equilibrium and we use the *Saha ionisation equation* [22, 24] to describe it:

$$\frac{x_e^2}{1 - x_e} = \frac{1}{n_e + n_H} \left(\frac{m_e T}{2\pi} \right)^{3/2} e^{-\epsilon/T} . \tag{2.79}$$

If we approximate $n_e + n_H \simeq n_b$ and multiply and divide the right hand side by the blackbody density of the photons, $n_\gamma = 2/\pi^2 \, T^3 \, \zeta(3)$, where $\zeta(3) \simeq 1.2021$, we obtain

$$\frac{x_e^2}{1 - x_e} \simeq 0.265 \, \frac{n_\gamma}{n_b} \left(\frac{m_e}{T} \right)^{3/2} e^{-\epsilon/T} . \tag{2.80}$$

The n_γ / n_b factor is the photon to baryon ratio, which is constrained by observations [39] to be equal to $\sim 1.64 \times 10^9$, while $\epsilon = 13.6\,\mathrm{eV}$ is the hydrogen ionisation energy.

The function $x_e(z)$ from the Saha equation is shown in Fig. 2.4. Due to the presence of the exponential term, we see that recombination is a sudden process. If we conventionally set the recombination temperature T_{rec} as the temperature when $x_e(T_{\mathrm{rec}}) = 0.5$, the Saha equation yields

$$T_{\mathrm{rec}} = 0.32\,\mathrm{eV} = 3700\,\mathrm{K} , \qquad \text{and} \qquad z_{\mathrm{rec}} = 1360 . \tag{2.81}$$

Because of the steep slope of the x_e curve, these values are not particularly sensitive to the choice of $x_e(T_{\mathrm{rec}})$. It should be noted that T_{rec} is considerably smaller than the energy needed to ionise an hydrogen atom. The reason is that the large value of n_γ / n_b pushes x_e to unity and significantly delays recombination; the photons are so abundant that, even at sub-eV energies, there are still enough of them in the high-energy tail of the Planck distribution to keep the Universe ionised [24].

The Saha equation is meant to be accurate only when recombination happens in quasi-equilibrium. In Fig. 2.4, we show the Saha solution together with the "exact" ionisation history as obtained from solving the Boltzmann equation. As expected, the Saha approximation is accurate in determining the redshift when recombination starts but it fails at lower redshifts when the system goes out of equilibrium. It should be noted that the x_e curve flattens at low redshift, as if recombination at some point

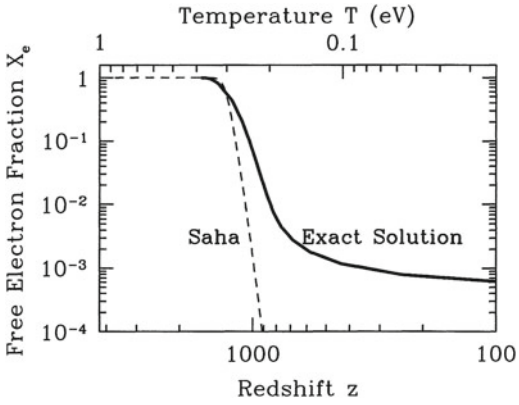

Fig. 2.4 Ionisation history of recombination. The free electron fraction is plotted against redshift and temperature. Recombination starts when x_e begins to drop and is a quick process. The Saha approximation (Eq. 2.80) correctly describes the beginning of recombination, but fails when the average energy of the photons becomes too small to maintain the $e + p \leftrightarrow H + \gamma$ reaction in equilibrium. Note that the exact solution does not drop to zero but, due to the reaction "freezing" when $\sigma_T \, x_e \, n_b \, c \ll H$, it asymptotes to $x_e \simeq 10^{-3}$. *Source* Dodelson [22, p. 72], reproduced with permission from Elsevier Books

had become ineffective in binding electrons and protons. This is indeed what happens after the recombination rate drops below the expansion rate, so that recombination "freezes" and the ionisation fraction remains constant.

2.5.2.2 Decoupling

Two particle species decouple from each other when their interaction rate drops below the cosmic expansion rate. Roughly speaking, if a photon scatters an electron less than once in an expansion time, equilibrium between the two species cannot be maintained. As we mentioned above, all the species are doomed to decouple at some point due to the expansion rate decreasing slower than any interaction rate. For the photons, the process of recombination anticipates this moment by suddenly removing most of the free electrons from the Universe.

We estimate the redshift of photon decoupling by equating the rate of photon scatterings with the cosmic expansion rate:

$$n_e(z_{\rm dec}) \, \sigma_T \, c \;=\; H(z_{\rm dec}). \tag{2.82}$$

Provided that we neglect the helium nuclei, we can express the fraction of free electrons as

$$n_e \;=\; x_e \, n_b \;=\; x_e \, \frac{\Omega_{b0} \, \rho_{\rm crit}}{m_p} \, (1+z)^3 \, .$$

where we have used $n_b = \rho_{b0}/m_p\, a^{-3}$. The Hubble parameter is given by the Friedmann equation Eq. 2.44,

$$H^2 = H_0^2\ (1+z)^3\ \Omega_{\rm M0}\left(1+\frac{1+z}{1+z_{\rm eq}}\right), \tag{2.83}$$

where we have neglected the cosmological constant and the curvature because they were insignificant at the high redshifts considered. By enforcing the condition in Eq. 2.82 we obtain

$$x_e\ (1+z_{\rm dec})^{3/2}\left(1+\frac{1+z_{\rm dec}}{1+z_{\rm eq}}\right)^{-1/2} = \left[\frac{m_p\, H_0\, \Omega_{\rm M0}^{1/2}}{c\,\rho_{\rm crit}\,\sigma_T\,\Omega_{b0}}\right]. \tag{2.84}$$

Inserting the cosmological parameters considered in Sect. 2.4.4, the term in the right hand side evaluates to 236 and $z_{\rm eq} \simeq 3380$. The ionisation fraction x_e needs to be computed numerically (Saha's equation is of no use when x_e is small) and we do so by using *RECFAST* [73]. This results in the values $z_{\rm dec} \simeq 900$ and $x_e(z_{\rm dec}) \simeq 10^{-2}$, which imply that photon decoupling takes place during recombination (recombination ends when the ionisation fraction reaches the freeze-out value of $x_e \simeq 10^{-3}$, see Fig. 2.4). It is interesting to note that if recombination did not happen the photons would have decoupled only at $z \simeq 40$; this can be seen by setting $x_e = 1$ in the above equation.

In Sect. 5.5 (and in SONG) we shall use a more sophisticated method to determine the time of photon decoupling, making use of the *visibility function*, the probability that a photon last scattered at a given redshift. In particular, we shall see that the visibility function peaks at $z_{\rm dec} \simeq 1100$, a redshift slightly higher than what we have inferred by enforcing $n_e\,\sigma_T\,c = H$. For a standard ΛCDM model, a redshift of $z_{\rm dec} \simeq 1100$ correponds to

$$\chi\,(z_{\rm dec}) \simeq 280\,{\rm Mpc}\ , \quad t\,(z_{\rm dec}) \simeq 380,000\,{\rm yr}\ , \quad T\,(z_{\rm dec}) \simeq 0.26\,{\rm eV}\ . \tag{2.85}$$

The three-dimensional spatial surface identified by the time of decoupling is called the *last scattering surface* (LSS). Note that the comoving particle horizon at the LSS, $\chi(z_{\rm dec}) \simeq 280\,{\rm Mpc}$, is roughly 80 times smaller than the one today, $\chi_0 \simeq 14200\,{\rm Mpc}$.

We conclude this section by noting that the electrons remain coupled to the photons even after recombination ends and the photons go out of thermal equilibrium. That is, the photons decouple from the electrons but not viceversa. This happens because the mean free path of an electron is much shorter than that of a photon, for the simple reason that there are many more photons than electrons. Equivalently, the interaction rate of the free electrons ($\sigma_T\, n_\gamma\, c$) is much larger than that of the photons ($\sigma_T\, x_e\, n_b\, c$) because $n_\gamma/n_b \gg 1$. Therefore, the temperature of the electrons does not decay as $1/a^2$, as it would be expected from a thermal fluid of massive particles, but follows that of the CMB until low redshifts.

2.6 Cosmic Inflation

The standard hot Big Bang model introduced in the previous sections succesfully accounts for the observed expansion of the Universe (Sect. 2.4.4), for the blackbody spectrum of the cosmic microwave background (Sect. 2.5) and for the abundances of the light nuclei created via nuclesynthesis (see, for example Refs. [22] and [24]). The model, however, is unable to answer several important observational and theoretical questions that we list below.

- **The Big Bang singularity** The most obvious issue is the presence of a a singularity in the finite past, the Big Bang (Sect. 2.4), when the curvature and the density of the Universe are divergent.
- **The Horizon problem** Any sign of correlations between regions of the Universe separated by a distance larger than the particle horizon cannot be explained by the standard model (Sect. 2.3.5). This is, however, what we observe: the cosmic microwave background has the same temperature with a precision of a part over 10^5 regardless of the direction of observation. The particle horizon at decoupling was 80 times smaller than the current value (Sect. 2.5.2.2), meaning that we would expect to observe fluctuations of order unity in the temperature of the CMB sky on angular scales of about 1°. The fact that we do not observe such fluctuations poses a causality problem that is referred to as the *horizon problem*: how can regions of the Universe be so similar if they did not have enough time to interact?
- **The Flatness problem** The Friedmann and acceleration equations (Eqs. 2.44 and 2.46) can be combined to obtain an evolution equation for the total density parameter $\Omega(t) \equiv \rho/\rho_{\rm crit} = 1 - k/(a^2H^2)$:

$$\frac{d}{dt}\Big[\,\Omega(t) - 1\,\Big] \;=\; \Big[\,\Omega(t) - 1\,\Big]\,\Omega(t)\;(1\,+\,3w)\;. \tag{2.86}$$

  This equation shows that, for a Universe with an equation of state of $w > -1/3$, such as in a mixture of matter and radiation, the solution $\Omega(t) = 1$ is dynamically unstable; in fact, the sign of the derivative is positive for $\Omega(t) > 1$ and negative for $\Omega(t) < 1$ so that $\Omega(t)$ will always evolve away from unity. This means that, for the Universe to be close to the critical density today as observations suggest, it had to be much more so in the past. For example, for a current value of $0.1 < \Omega_0 < 2$, it can be shown [24] that $|\Omega - 1| \leq 10^{-15}$ at nucleosynthesis ($z \simeq 10^9$) and $|\Omega - 1| \leq 10^{-60}$ at the Planck time ($t_P = \sqrt{\hbar G/c^5} \simeq 5.4\times10^{-44}$ s). The smallness of these values poses a fine-tuning issue that is called the *flatness problem*: how can the Universe be still so close to the critical density?
- **The structure problem** We observe tiny anisotropies in the CMB with an amplitude of $\Delta T/T \approx 10^5$ and, more evidently, the observed Universe is highly inhomogeneous with a strongly clustered distribution of galaxies on small scales. By which mechanism was this structure formed?

These shortcomings of the hot Big Bang model are all connected to the initial conditions of the Universe. In this section we shall see that, apart from the Big Bang

singularity, they can be solved by postulating the existence of a phase of accelerated expansion in the early Universe, the so-called *cosmic inflation*. We first describe in Sect. 2.6.1 how inflation solves the aforementioned cosmological problems. Then, in Sect. 2.6.2 we show that the inflationary expansion can be achieved if the early Universe was dominated by a slowly-evolving scalar field, the so-called inflaton. In section Sect. 2.6.3 we briefly discuss how inflation generates the density fluctuations that have seeded the observed structure on large scales. In particular, we shall focus on the possibility that these primordial fluctuations are non-Gaussian, thus opening a window on interesting new physics. (Note that to do so we use the concepts of cosmological perturbations and n-point functions, which are described only in the next chapter.)

In this section we shall only mention the fundamental properties of inflation. A detailed description of the topic can be found in several textbooks. For example, Chap. 6 of Dodelson [22] provides a pedagogical introduction to inflation while Liddle and Lyth [47] treat inflation from a more advanced point of view; we refer the reader to these references for the omissions of this section. Technical reviews focussed on the generation of non-Gaussianity during inflation can be found in Refs. [8, 15].

2.6.1 The Accelerated Expansion

The mechanism of cosmic inflation [2, 33, 50, 77] consists of postulating the existence of a period in which the Universe was much smaller than what one would infer based on the standard Big Bang model. In this period, the same regions of the Universe that we see today as separate and independent, were actually in causal contact. In order to link this "small universe" with the size of the universe today, one needs to postulate a phase in between where the Universe has expanded much quicker than the normal rate; hence the name cosmic inflation. In Fig. 2.5 we explain this process in terms of a conformal diagram of cosmic inflation.

Cosmic inflation solves the horizon problem by connecting regions that, in a standard Big Bang model, would be causally disconnected. For this to happen, the comoving Hubble radius, which we defined in Sect. 2.3.5 to be $c/(aH)$, at the beginning of inflation had to be larger than the largest scale observable today, that is the current comoving Hubble radius. Since after inflation the horizon grows with time (Sect. 2.4.4), it follows that during inflation it has to decrease; the expansion during inflation must therefore satisfy

$$\frac{d}{dt}\left[\frac{1}{aH}\right] < 0 \quad \Rightarrow \quad \frac{d^2a}{dt^2} > 0\,, \tag{2.87}$$

that is, the expansion had to be *accelerated*. It is important to remark that it is not the accelerated expansion that solves the horizon problem: the causal connection (i.e. the

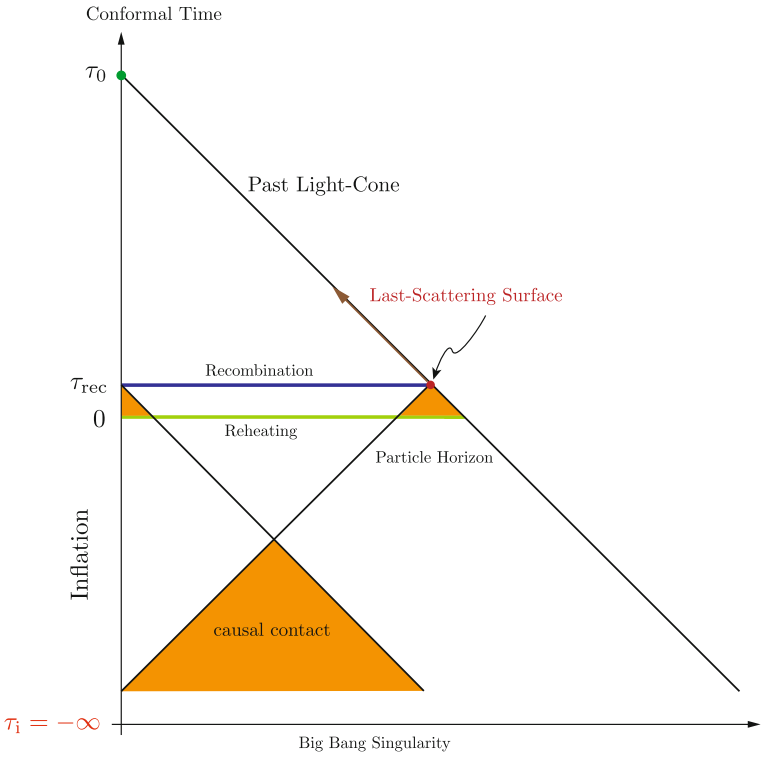

Fig. 2.5 Conformal diagram of inflation. The y-axis is conformal time, while the x-axis is distance. Our vantage point is today (τ_0), on the $x = 0$ vertical line. The standard Big Bang model predicts that the dynamical evolution of the Universe started at $\tau = 0$ (*green horizontal line*). In this picture, the past light cones of two distant CMB patches (*small orange triangles*) do not intersect, because the particle horizon at the time where the CMB is formed (*horizontal line* at $\tau_{\rm rec}$) is much smaller than τ_0. Therefore, we expect order-unity differences in the CMB temperature on large scales. However, we observe the CMB today to be almost perfectly isotropic on all scales; this is the horizon problem. In the inflationary scenario, the horizon problem is solved by postulating the existence of a period where the two CMB patches were in casual contact (*big orange triangle*). This is achieved by extending the time axis below $\tau = 0$ in order to allow the past-light cones of the two CMB patches to intersect. A period of accelerated expansion, *cosmic inflation*, is needed in order to bridge the gap between the "small Universe" where the casual contact was established, and the large value of today's particle horizon. In this context, $\tau = 0$ is not a singularity but an apparent Big Bang, as it marks the end of inflation and the decay of the inflaton (Sect. 2.6.2) into a thermal mix of elementary particles. The actual Big Bang singularity sits at $\tau \to -\infty$. *Source* Courtesy of Daniel Baumann, from Fig. 9 of Baumann [10]

Universe becoming uniform) is established *before inflation* and what inflation does is to put those regions out of reach again, because this is how we see them today.

The accelerated expansion, however, does solve the flatness problem, because it washes out any curvature, stretching the geometry of the Universe so much that

it becomes spatially flat [38]. More quantitatively, we see from the acceleration equation (Eq. 2.46),

$$\frac{a''}{a} \;=\; -\frac{4\,\pi\,G}{3}\;(\rho \;+\; 3\,P)\;, \tag{2.88}$$

that the Universe undergoes an accelerated expansion only if $\rho + 3\,P \;<\; 0$ or, in terms of the barotropic parameter, if $w < -\frac{1}{3}$. If we inspect Eq. 2.86, we realise that this is the same condition needed to make $\Omega(t) = 1$ an attractor solution; that is, if cosmic inflation lasted long enough, the flatness problem would be solved without the need to fine tune the initial curvature. In fact, we can ask the question: how many times must the Universe double in size during inflation to justify the fact that today's Universe is so close to the critical density? The answer comes from the Friedmann equation for a constant equation of state (Eq. 2.44):

$$|\Omega(t) - 1| \;=\; \frac{3\,|k|}{8\,\pi\,G\,a^2\,\rho} \;\propto\; a^{1+3\,w}\;. \tag{2.89}$$

If we assume that during the inflationary phase $w = -1$, then $|\Omega(t) - 1|$ decreases like a^{-2}; to bring $|\Omega(t) - 1|$ to today's value of order unity from $\sim 10^{-60}$ at the Planck time would require that

$$N \;\equiv\; \ln\left(\frac{a_{\rm end}}{a_{\rm ini}}\right) \;\simeq\; 30\;\ln(10) \;\simeq\; 70\;, \tag{2.90}$$

where N is called the number of e-foldings and $a_{\rm ini}$ and $a_{\rm end}$ mark the beginning and the end of inflation, respectively.

Cosmic inflation provides a solution to the structure problem that is rooted in quantum mechanics; we postpone this discussion until Sect. 2.6.3.

2.6.2 Single Field Model

Inflation is a mechanism rather than a theory of the early Universe, a phase of accelerated expansion before which the comoving horizon was larger than the largest scale observable today. We have seen that to realise the accelerated expansion it is necessary for the matter content of the Universe to have an equation of state of $w < -\frac{1}{3}$, which corresponds to a negative pressure, $\rho + 3\,P \;<\; 0$. Neither cold matter ($w = 0$) nor radiation ($w = \frac{1}{3}$) are suitable candidates as they have positive pressure; the cosmological constant ($w = -1$) can produce an accelerated expansion but is completely negligible in the early Universe, so it cannot be responsible for inflation.

Let us see how the presence of a *scalar field*, which we call the *inflaton* ϕ, can trigger the mechanism of cosmic inflation. The scalar field Lagrangian is given by

$$\mathcal{L}_\phi \;=\; -\frac{1}{2}\,\partial_\mu\,\phi\,\partial^\mu\,\phi \;-\; V(\phi)\;, \tag{2.91}$$

where $V(\phi)$ is the potential for the field, which we assume to be positive. In principle $\mathcal{L}$ should include terms to account for the interactions with the other species, but we postulate that they are negligible during inflation. The pressure and the energy density of the inflaton field can be inferred from its energy-momentum tensor:

$$T_{\mu\nu} \;=\; \partial_\mu\,\phi\,\partial_\nu\,\phi \;-\; \frac{1}{2}\,g_{\mu\nu}\,\partial_\alpha\,\phi\,\partial^\alpha\,\phi \;-\; g_{\mu\nu}\,V(\phi)\;. \tag{2.92}$$

Here we assume that the Universe is homoegenous, so that $g_{\mu\nu}$ is the conformal *FLRW* metric in Eq. 2.16 and the spatial gradients of ϕ vanish. It follows that

$$\rho_\phi \;=\; -T^0{}_0 \;=\; \frac{1}{2}\,\phi'^2 \;+\; V(\phi) \quad \text{and} \quad P_\phi \;=\; \frac{1}{3}\,T^i{}_i \;=\; \frac{1}{2}\,\phi'^2 \;-\; V(\phi)\;. \tag{2.93}$$

where $\phi' \;=\; d\phi/dt$. The expression for the energy density is reminiscent of that of a particle moving in a potential V with velocity ϕ' and kinetic energy $\frac{1}{2}\,\phi'^2$. In this picture, a field with negative pressure is one with more potential energy than kinetic. In the limit where the inflaton field is constant ($\phi' = 0$), its kinetic energy vanishes and we have a constant energy density: $\rho_\phi \;=\; V(\phi) \;=\;$ constant. If we assume that the energy density and pressure of the Universe are dominated by the inflaton's contribution, the expansion rate of the Universe is determined by ρ_ϕ via the Friedmann equation Eq. 2.39:

$$H \;=\; \frac{1}{a}\,\frac{da}{dt} \;=\; \sqrt{\frac{8\,\pi\,G\,\rho_\phi}{3}} \;=\; \text{constant}\;, \tag{2.94}$$

It follows that a Universe whose dynamical evolution is determined by a *constant* scalar field expands at an exponential rate: $a \;\propto\; e^{H\,t}$, where $H \;\propto\; \sqrt{\rho_\phi}$ constant. Inflation is therefore realised.

The Friedmann equation (Eq. 2.39) during inflation reads

$$H^2 \;=\; \frac{1}{3\,m_{\rm P}^2}\,\left(\frac{1}{2}\,\phi'^2 \;+\; V(\phi)\right)\;, \tag{2.95}$$

where we have introduced the Planck mass $m_{\rm P} \;\equiv\; (8\pi G)^{-1/2} \;\simeq\; 2.4 \times 10^{18}\,\text{GeV}$. The Friedmann and acceleration (Eq. 2.46) equations can be combined to yield the background evolution of the inflaton,

$$\phi'' \;+\; 3\,H\,\phi' \;+\; V_{,\phi} \;=\; 0\;, \tag{2.96}$$

where the primes denote derivatives with respect to cosmic time t and $V_{,\phi} = \partial V/\partial\phi$.

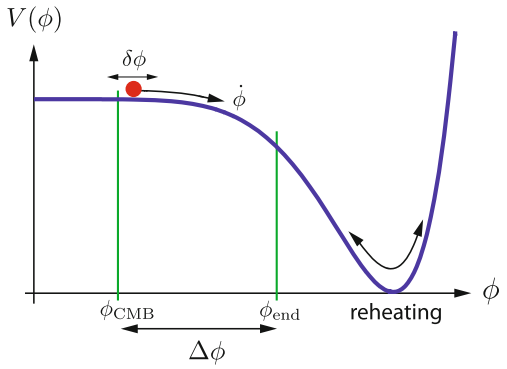

Fig. 2.6 Example of a slow-roll inflationary potential. As long as the inflaton's kinetic energy, $\frac{1}{2}\,\phi'^2$, is negligible with respect to its potential energy, $V(\phi)$, the Universe expands in an accelerated fashion; this limit corresponds to the constant part of the potential. When $\frac{1}{2}\,\phi'^2 \simeq V(\phi)$, the acceleration can no longer be sustained and inflation ends. When the inflaton reaches the minimum of the potential, reheating occurs and the energy density of the inflaton is converted into a thermal mix of elementary particles. *Source* Courtesy of Daniel Baumann, from Fig. 10 of Baumann [10]

2.6.2.1 The Slow-Roll Condition

We have just proved that a scalar field can drive inflation as long as it does not evolve significantly, $\phi'^2 \ll V(\phi)$. The issue now is to determine the potential $V(\phi)$ that keeps ϕ nearly constant for the number of e-foldings necessary to solve the horizon and flatness problems. Most models of inflation satisfy the *slow-roll condition* [2, 50], whereby the inflaton stays nearly constant by slowly rolling down a potential that is almost flat. We show an example of a slow-roll potential in Fig. 2.6. Because inflation cannot last forever, the potential needs to have a minimum; as time goes on, the inflaton approaches this minimum and, due to the increased slope of the potential, it starts to evolve faster. Inflation comes to an end when the kinetic energy $\frac{1}{2}\,\phi'^2$ grows to be of the order of the potential $V(\phi)$. When the inflaton eventually reaches the minimum of the potential, the coupling with the other fields becomes significant so that it decays into a thermal mix of elementary particles [24], leading to a radiation dominated universe in a process called *reheating*. In practice, we can think of the reheating process after inflation as the moment when the hot Big Bang occurs, in which matter and radiation as we know them start to be created.

Many different potentials can be devised that satisfy the slow-roll condition. It is customary to parametrise them with two variables that vanish in the limit where ϕ is constant. The first slow-roll parameter η quantifies the variation in the Hubble factor, and is related to the first derivative of the inflaton potential. It is defined as

$$\epsilon \equiv \frac{d}{dt}\left(\frac{1}{H}\right) = -\frac{H'}{H^2} \approx \frac{m_P^2}{2}\left(\frac{V_{,\phi}}{V}\right)^2 . \tag{2.97}$$

Whenever the inflaton field is constant, $\phi' = 0$, then also $H \propto \sqrt{\rho_\phi}$ is constant (Eq. 2.94) meaning that the ϵ parameter vanishes. In fact, the slow-roll condition requires $\epsilon \ll 1$, an assumption that implies an approximate time-translation invariance of the background. On the other hand, in the radiation dominated era $\epsilon = 2$; in fact, one can define the inflationary epoch as $\epsilon < 1$. The second slow-roll parameter, η, is directly related to the second derivative of the potential,[10]

$$\eta \equiv m_P^2 \left(\frac{V_{,\phi\phi}}{V}\right) . \tag{2.99}$$

Again, in the case of a constant field or potential this parameter vanishes. As we shall see below, the most important predictions of inflation can be recast in terms of the slow-roll parameters ϵ and η.

2.6.3 Primordial Fluctuations

Cosmic inflation was originally proposed to solve the horizon and flatness problems [2, 33, 50, 77], but it was soon realised that it also provided a mechanism to generate primordial density fluctuations [7, 37, 59, 78]. The idea is that the structure that we observe today, such as the CMB anisotropies and the galaxy distribution, formed starting from tiny quantum fluctuations set during inflation and later enhanced throughout cosmic history via gravitational instability. These primordial fluctuations were generated as microscopic quantum vacuum fluctuations in the inflaton field that, during inflation, were stretched and imprinted on superhorizon scales by the accelerated expansion. These density fluctuations reentered the horizon after inflation ended and served as initial conditions for the anisotropy and the growth of structure in the Universe.

In what follows, we briefly describe the main features of the primordial fluctuations generated during inflation. To do so, we need to use some concepts that will be formally defined only in the next chapter, like the idea that the primordial fluctuations generated during inflation are stochastic in nature and, therefore, their magnitude is determined in terms of their variance (in real space) or their power spectrum (in Fourier space). We will also use of the concepts of scalar and tensor (Sect. 3.3.1) perturbations (Sect. 3.4), power spectrum (Sect. 3.7.1) and bispectrum (Sect. 3.7.2).

[10] In defining the slow-roll parameters, we are using the notation of the review by Bartolo et al. [8]. Chen [15], on the other hand, denotes the quantity in Eq. 2.99 as η_V and uses the symbol η for a third slow-roll parameter:

$$\eta \equiv -2\eta_V + 4\epsilon = \frac{\epsilon'}{\epsilon H} . \tag{2.98}$$

.

2.6.3.1 Scalar Fluctuations

The primordial fluctuations generated during slow-roll inflation are expected to have nearly the same variance on all spatial scales. The reason is that the slow-roll condition $\epsilon = -H'/H^2 \ll 1$ results into an approximate time-translation invariance of the background. Therefore, the primordial fluctuations are produced with approximately the same background expansion rate regardless of the scale considered. This *scale invariance* is usually quantified in terms of the *scalar spectral index*, n_s, defined to be the slope of the *dimensionless power spectrum* of the primordial curvature perturbation,

$$\mathcal{P}_{\mathcal{R}} \propto k^{n_s - 1} . \tag{2.100}$$

The condition of scale invariance translates to $n_s = 1$. However, the presence of structure in the inflaton potential affects the expansion rate and, therefore, it generates deviations from scale invariance. In a slow-roll inflationary model where the potential is nearly flat, these deviations are small [8, 15]:

$$n_s = 1 - 6\epsilon + 2\eta . \tag{2.101}$$

Because the slow-roll parameters ϵ and η describe, respectively, the first and second derivative of the inflaton potential $V(\phi)$, measuring n_s is equivalent to constraining the shape of $V(\phi)$. The cosmic microwave background is strongly affected by the tilt of the primordial fluctuations and, as a result, it can be used to constrain n_s [67]:

$$n_s = 0.9603 \pm 0.0073 \qquad \text{at } 68\,\% \text{ confidence level} . \tag{2.102}$$

This measurement is in agreement with the slow-roll inflationary models and suggests that the two slow-roll parameters have a value of $\mathcal{O}(10^{-2})$.

Another important observable of inflation is the amplitude A_s of the primordial fluctuations, which is defined as

$$\mathcal{P}_{\mathcal{R}}(k) = A_s \left(\frac{k}{k_0}\right)^{n_s - 1} , \tag{2.103}$$

where k_0 is the pivot scale. In the slow-roll limit, the amplitude A_s is connected to the ratio between the inflaton potential and the slow-roll parameter ϵ [68]:

$$A_s = \frac{V}{24\,\pi^2\, m_P^4\, \epsilon} . \tag{2.104}$$

By measuring the amplitude of the CMB angular spectrum, the Planck team [68] found the value $\ln(10^{10}\, A_s) = 3.089^{+0.024}_{-0.027}$ at 68 % confidence level for a pivot scale

of $k_0 = 0.05\,\mathrm{Mpc}^{-1}$, which translates to a constraint on the energy scale of inflation, $V^{1/4}$, and on ϵ:

$$\frac{V^{1/4}}{\epsilon^{1/4}} \;=\; 0.027\, m_\mathrm{P} \;=\; 6.6 \times 10^{16}\,\mathrm{GeV}\,. \tag{2.105}$$

2.6.3.2 Gravitational Waves

Another prediction from inflation is the presence of a background of primordial gravitational waves. These are generated with the same mechanism as the scalar fluctuations and are thus also expected to be nearly scale invariant. The power spectrum of tensor fluctuations,

$$\mathcal{P}_t(k) \;=\; A_t \left(\frac{k}{k_0}\right)^{n_t}\,, \tag{2.106}$$

defines the tensor amplitude A_t and the *tensor spectral index* n_t, which vanishes for a scale-invariant spectrum. For a slowly rolling scalar field, they are given by [22, 68]

$$A_t \;=\; \frac{2\,V}{3\,\pi^2\, m_\mathrm{P}^4}\,, \qquad \text{and} \qquad n_t = -2\,\epsilon\,. \tag{2.107}$$

In the slow-roll limit, a *consistency relation* links the spectral index n_t to the amplitudes of the scalar and tensor power spectra:

$$r \;\equiv\; \frac{\mathcal{P}_t}{\mathcal{P}_\mathcal{R}} \;=\; -8\,n_t\,, \tag{2.108}$$

where we have defined the *tensor-to-scalar ratio* r. Since A_s has already been experimentally determined, measuring the value of r would automatically yield the amplitude of the tensor perturbations A_t and, through the consistency relation, the tilt n_t of the tensor spectrum. Furthermore, a determination of r would imply also an indirect detection of the gravitational waves. So far, only upper limits for the tensor-to-scalar exist; in Fig. 2.7 we show the joint measurement of r and n_s produced by the Planck experiment [68].

2.6.4 Non-Gaussianity

The inflation observables that we have introduced in the previous subsection, the spectral index n_s and the tensor-to-scalar ratio r, are defined with respect to the power spectrum of the primordial curvature perturbation, $\mathcal{P}_\mathcal{R}$. The power spectrum,

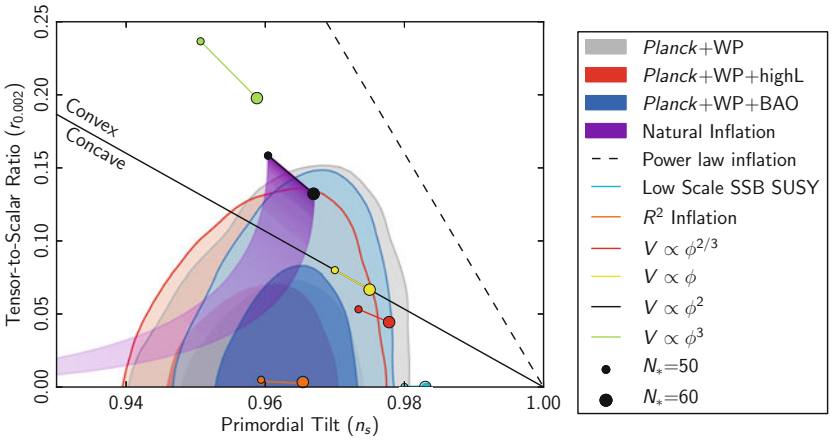

Fig. 2.7 Constraints on the spectral tilt and the tensor-to-scalar ratio r from Planck [68]. The ellipses represent the 68 and 95 % confidence limits on n_s and r for various combinations of datasets (*WP* WMAP polarisation, *BAO* Baryon acoustic oscillation, *highL* high-resolution CMB data). The theoretical predictions of several inflationary models are also shown. Credit: Fig. 1 on p.10 of Ref. [68] by the Planck collaboration, A&A, reproduced with permission © ESO

however, is just one of the infinite series of n-point functions that characterise the primordial field (Sect. 3.4). In the case of a Gaussian random field, these moments can be expressed as products of $\mathcal{P}_\mathcal{R}$; for an arbitrary field, this is not the case: the higher-order moments contain extra information that eludes the power spectrum and that, as we shall soon see, is precious to understand the non-linear physics at work in the early Universe. We shall refer to this extra information as *non-Gaussianity*, simply because it is absent for Gaussian perturbations.

In this thesis, we focus on the three-point function of the primordial curvature perturbation, or *primordial bispectrum*. The full formalism to characterise the bispectrum and its observability in the cosmic microwave background will be introduced in Chap. 6. The purpose of this subsection is to explain our motivations for studying the bispectrum; therefore, for now, we shall keep the technical details to a minimum.

The primordial bispectrum is important for two reasons. First, it is the lowest order statistic sensitive to whether a perturbation is Gaussian or non-Gaussian. This follows from the fact that the three-point function of a Gaussian random field with zero mean vanishes. Secondly, it is directly related to the angular bispectrum of the cosmic microwave background, which is an observable quantity [42, 43, 85]. Therefore, the primordial bispectrum as inferred from the CMB has the power of discriminating models of inflation based on the amount of non-Gaussianity they produce.

The standard slow-roll inflation models that we have described above, where the accelerated expansion is driven by a non-interacting scalar field, produce a bispectrum of the order of the slow-roll parameters [1, 53]; for all practical purposes, this non-Gaussianity can be considered negligible. This is intuitive as the bispectrum is inherently related to the non-linearities in the propagation of the field. In the "vanilla"

models, the inflaton propagates freely along a very flat potential ($\epsilon, |\eta| \ll 1$), so that any self-interaction term of the inflaton potential and the gravitational coupling must be very small; consequently, the non-linearities are also suppressed [8].

Measuring a significant bispectrum would therefore rule out the simplest models of inflation. It should be stressed that these models are otherwise highly successful in reproducing the required duration of inflation and the observed shape of the power spectrum. The non-Gaussianity measurement is thus complementary to the usual inflation observables, n_s and r, and it provides extra information on the physics of the early Universe that is useful to break degeneracies between models that would otherwise be observationally equivalent.

The constraining power of the primordial bispectrum and its observability prompted particle physicists and cosmologists to join forces and investigate many well-motivated extensions to the inflationary vanilla model. The multiple-field models, for example, postulate that two or more fields are present during inflation. These models are appealing also because, from the point of view of particle physics, it is natural to have several other fields that contribute to the inflationary dynamics. If the fields interact, the Lagrangian will include non-linear contributions that ultimately lead to deviations from pure Gaussian statistics [8, 13, 74]. This is not, however, the only mechanism to create non-Gaussianity in a multi-field model. In the *curvaton scenario* [28, 49, 51, 56, 57], for example, the inflaton field drives the accelerated expansion as in a single field model, while a subdominant second field, the curvaton, is responsible for generating the curvature perturbations. In this case, the non-Gaussianity is produced by the non-linear evolution of the curvature perturbation on superhorizon scales.

Other extensions to the vanilla model include features in the inflaton potential, the presence of a non-canonical kinetic term, non-linearities in the initial vacuum state or modifications to the theory of gravity [15]. These features generally translate to non-Gaussian signatures in the primordial curvature perturbation and, thus, in specific shapes of the bispectrum. For a review on these models and their observability, refer to the reviews in Refs. [9, 42, 48, 85].

In summary, the non-Gaussianity of the cosmological perturbations opens a window on the non-linear physics of the early Universe; the CMB bispectrum is the observable that allows us to look through this window. The subject of this thesis is the connection between the primordial non-Gaussianity and the CMB bispectrum. In the following chapters, we shall answer the questions: how is the measured CMB bispectrum affected by the non-linear evolution that happens *after* inflation? Would this effect significantly bias a measurement of the primordial signal?

The answers can be found in Chap. 6.

References

1. Acquaviva V, Bartolo N, Matarrese S, Riotto A (2003) Gauge-invariant second-order perturbations and non-Gaussianity from inflation. Nucl Phys B 667:119–148. doi:10.1016/S0550-3213(03)00550-9. arXiv:astro-ph/0209156
2. Albrecht A, Steinhardt PJ (1982) Cosmology for grand unified theories with radiatively induced symmetry breaking. Phys Rev Lett 48:1220–1223. doi:10.1103/PhysRevLett.48.1220
3. Ali-Haïmoud Y, Hirata CM (2010) Ultrafast effective multilevel atom method for primordial hydrogen recombination. Phys Rev D 82(6):063521. doi:10.1103/PhysRevD.82.063521. arXiv:1006.1355
4. Ali-Haïmoud Y, Hirata CM (2011) HyRec: a fast and highly accurate primordial hydrogen and helium recombination code. Phys Rev D 83(4):043513. doi:10.1103/PhysRevD.83.043513. arXiv:1011.3758
5. Alonso D, Bueno Belloso A, Sánchez FJ, García-Bellido J, Sánchez E (2014) Measuring the transition to homogeneity with photometric redshift surveys. MNRAS 440:10–23. doi:10.1093/mnras/stu255. arXiv:1312.0861
6. Amendola L, Tsujikawa S (2010) Dark energy: theory and observations. Cambridge University Press, Cambridge
7. Bardeen JM, Steinhardt PJ, Turner MS (1983) Spontaneous creation of almost scale-free density perturbations in an inflationary universe. Phys Rev D 28:679–693. doi:10.1103/PhysRevD.28.679
8. Bartolo N, Komatsu E, Matarrese S, Riotto A (2004) Non-Gaussianity from inflation: theory and observations. Phys Rep 402:103–266. doi:10.1016/j.physrep.2004.08.022. arXiv:astro-ph/0406398
9. Bartolo N, Matarrese S, Riotto A (2010) Non-gaussianity and the cosmic microwave background anisotropies. Adv Astron. doi:10.1155/2010/157079. arXiv:1001.3957
10. Baumann D (2009) TASI lectures on inflation. arXiv:0907.5424
11. Bennett CL, Banday AJ, Gorski KM, Hinshaw G, Jackson P, Keegstra P, Kogut A, Smoot GF, Wilkinson DT, Wright EL (1996) Four-year COBE DMR cosmic microwave background observations: maps and basic results. Astrophys J Lett 464:L1+. doi:10.1086/310075. arXiv:astro-ph/9601067
12. Bunker AJ, Caruana J, Wilkins SM, Stanway ER, Lorenzoni S, Lacy M, Jarvis MJ, Hickey S (2013) VLT/XSHOOTER and Subaru/MOIRCS spectroscopy of HUDF.YD3: no evidence for Lyman α emission at z = 8.55. MNRAS 430:3314–3319. doi:10.1093/mnras/stt132. arXiv:1301.4477
13. Byrnes CT, Choi KY (2010) Review of local non-gaussianity from multifield inflation. Adv Astron doi:10.1155/2010/724525. arXiv:1002.3110
14. Caldwell RR, Stebbins A (2008) A test of the Copernican principle. Phys Rev Lett 100(19):191302. doi:10.1103/PhysRevLett.100.191302. arXiv:0711.3459
15. Chen X (2010) Primordial non-gaussianities from inflation models. Adv Astron 2010:638979. doi:10.1155/2010/638979. arXiv:1002.1416
16. Clarkson C (2012) Establishing homogeneity of the universe in the shadow of dark energy. Comptes Rendus Physique 13:682–718. doi:10.1016/j.crhy.2012.04.005. arXiv:1204.5505
17. Clifton T, Ferreira PG, Zuntz J (2009) What the small angle CMB really tells us about the curvature of the Universe. J Cosmol Astropart Phys 7:029. doi:10.1088/1475-7516/2009/07/029. arXiv:0902.1313
18. Colless M, Dalton G, Maddox S, Sutherland W, Norberg P, Cole S, Bland-Hawthorn J, Bridges T, Cannon R, Collins C, Couch W, Cross N, Deeley K, De Propris R, Driver SP, Efstathiou G, Ellis RS, Frenk CS, Glazebrook K, Jackson C, Lahav O, Lewis I, Lumsden S, Madgwick D, Peacock JA, Peterson BA, Price I, Seaborne M, Taylor K (2001) The 2dF Galaxy Redshift Survey: spectra and redshifts. MNRAS 328:1039–1063. doi:10.1046/j.1365-8711.2001.04902.x. arXiv:astro-ph/0106498
19. Davis M (1997) Is the universe homogeneous on large scales? In: Turok N (ed) Critical dialogues in cosmology, p 13

20. Dawson KS, Schlegel DJ et al (2013) The Baryon oscillation spectroscopic survey of SDSS-III. AJ 145:10. doi:10.1088/0004-6256/145/1/10. arXiv:1208.0022
21. Dicke RH, Peebles PJE, Roll PG, Wilkinson DT (1965) Cosmic black-body radiation. Astrophys J 142:414–419. doi:10.1086/148306
22. Dodelson S (2003) Modern cosmology. Academic Press, New York
23. Drinkwater MJ, Jurek RJ, Blake C, Woods D, Pimbblet KA et al (2010) The WiggleZ Dark Energy Survey: survey design and first data release. MNRAS 401:1429–1452. doi:10.1111/j.1365-2966.2009.15754.x. arXiv:0911.4246
24. Durrer R (2008) The cosmic microwave background. Cambridge University Press, Cambridge
25. Durrer R, Eckmann JP, Sylos Labini F, Montuori M, Pietronero L (1997) Angular projections of fractal sets. Europhys Lett 40:491–496. doi:10.1209/epl/i1997-00493-3. arXiv:astro-ph/9702116
26. Ellis GFR (1975) Cosmology and verifiability. QJRAS 16:245–264
27. Ellis RS, McLure RJ, Dunlop JS, Robertson BE et al (2013) The abundance of star-forming galaxies in the redshift range 8.5–12: new results from the 2012 Hubble ultra deep field campaign. ApJ 763:L7. doi:10.1088/2041-8205/763/1/L7. arXiv:1211.6804
28. Enqvist K, Sloth MS (2002) Adiabatic CMB perturbations in pre-Big-Bang string cosmology. Nucl Phys B 626:395–409. doi:10.1016/S0550-3213(02)00043-3. arXiv:hep-ph/0109214
29. Finkelstein SL, Papovich C, Dickinson M, Song M, Tilvi V et al (2013) A galaxy rapidly forming stars 700 million years after the Big Bang at redshift 7.51. Nature 502:524–527. doi:10.1038/nature12657. arXiv:1310.6031
30. Fixsen DJ, Cheng ES, Gales JM, Mather JC, Shafer RA, Wright EL (1996) The cosmic microwave background spectrum from the Full COBE FIRAS data set. Astrophys J 473:576. doi:10.1086/178173. arXiv:astro-ph/9605054
31. Freedman WL, Madore BF, Scowcroft V, Burns C, Monson A, Persson SE, Seibert M, Rigby J (2012) Carnegie Hubble program: a mid-infrared calibration of the Hubble constant. ApJ 758:24. doi:10.1088/0004-637X/758/1/24. arXiv:1208.3281
32. Friedmann A (1922) Über die Krümmung des Raumes. Zeitschrift fur Physik 10:377–386. doi:10.1007/BF01332580
33. Guth AH (1981) Inflationary universe: a possible solution to the horizon and flatness problems. Phys Rev D 23(2):347–356. doi:10.1103/PhysRevD.23.347
34. Guzzo L (1997) Is the universe homogeneous? (On large scales). New Astron 2:517–532. doi:10.1016/S1384-1076(97)00037-7. arXiv:astro-ph/9711206
35. Hamilton JC (2013) What have we learned from observational cosmology? In: Proceedings of "Philosophical Aspects of Modern Cosmology" held in Granada, Spain, 2011. arXiv:1304.4446
36. Harrison ER (2000) Cosmology. The science of the universe. Cambridge University Press, Cambridge
37. Hawking SW (1982) The development of irregularities in a single bubble inflationary universe. Phys Lett B 115:295–297. doi:10.1016/0370-2693(82)90373-2
38. Hawley JF, Holcomb KA (2005) Foundations of modern cosmology, 2nd edn. Oxford Univerxity Press, Oxford
39. Hinshaw G, Larson D, Komatsu E, Spergel DN, Bennett CL, Dunkley J, Nolta MR, Halpern M, Hill RS, Odegard N, Page L, Smith KM, Weiland JL, Gold B, Jarosik N, Kogut A, Limon M, Meyer SS, Tucker GS, Wollack E, Wright EL (2013) Nine-year Wilkinson Microwave Anisotropy Probe (WMAP) observations: cosmological parameter results. ApJS 208:19. doi:10.1088/0067-0049/208/2/19. arXiv:1212.5226
40. Hogg DW, Eisenstein DJ, Blanton MR, Bahcall NA, Brinkmann J, Gunn JE, Schneider DP (2005) Cosmic homogeneity demonstrated with luminous red galaxies. Astrophys J 624:54–58. doi:10.1086/429084. arXiv:astro-ph/0411197
41. Hubble E (1929) A relation between distance and radial velocity among extra-galactic nebulae. Proc Natl Acad Sci 15:168–173. doi:10.1073/pnas.15.3.168
42. Komatsu E (2010) Hunting for primordial non-Gaussianity in the cosmic microwave background. Class Quantum Gravity 27(12):124,010. doi:10.1088/0264-9381/27/12/124010. arXiv:1003.6097

43. Komatsu E, Spergel DN (2001) Acoustic signatures in the primary microwave background bispectrum. Phys Rev D 63(6):063002. doi:10.1103/PhysRevD.63.063002. arXiv:astro-ph/0005036
44. Lehnert MD, Nesvadba NPH, Cuby JG, Swinbank AM, Morris S, Clément B, Evans CJ, Bremer MN, Basa S (2010) Spectroscopic confirmation of a galaxy at redshift z = 8.6. Nature 467:940–942. doi:10.1038/nature09462. arXiv:1010.4312
45. Lemaître G (1927) Un Univers homogène de masse constante et de rayon croissant rendant compte de la vitesse radiale des nébuleuses extra-galactiques. Annales de la Societe Scietifique de Bruxelles 47:49–59
46. Lemaître G (1931) Expansion of the universe, a homogeneous universe of constant mass and increasing radius accounting for the radial velocity of extra-galactic nebulae. MNRAS 91:483–490
47. Liddle AR, Lyth DH (2000) Cosmological inflation and large-scale structure. Cambridge University Press, Cambridge
48. Liguori M, Sefusatti E, Fergusson JR, Shellard EPS (2010) Primordial non-gaussianity and bispectrum measurements in the cosmic microwave background and large-scale structure. Adv Astron doi:10.1155/2010/980523. arXiv:1001.4707
49. Linde A, Mukhanov V (1997) Non-Gaussian isocurvature perturbations from inflation. Phys Rev D 56:535. doi:10.1103/PhysRevD.56.R535. arXiv:astro-ph/9610219
50. Linde AD (1982) A new inflationary universe scenario: a possible solution of the horizon, flatness, homogeneity, isotropy and primordial monopole problems. Phys Lett B 108:389–393. doi:10.1016/0370-2693(82)91219-9
51. Lyth DH, Wands D (2002) Generating the curvature perturbation without an inflaton. Phys Lett B 524:5–14. doi:10.1016/S0370-2693(01)01366-1. arXiv:hep-ph/0110002
52. Maartens R (2011) Is the universe homogeneous? Roy Soc Lond Philos Trans Ser A 369:5115–5137. doi:10.1098/rsta.2011.0289. arXiv:1104.1300
53. Maldacena J (2003) Non-gaussian features of primordial fluctuations in single field inflationary models. J High Energy Phys 5:13. doi:10.1088/1126-708/2003/05/013. arXiv:astro-ph/0210603
54. Mather JC, Cheng ES, Cottingham DA, Eplee RE Jr, Fixsen DJ, Hewagama T, Isaacman RB, Jensen KA, Meyer SS, Noerdlinger PD, Read SM, Rosen LP, Shafer RA, Wright EL, Bennett CL, Boggess NW, Hauser MG, Kelsall T, Moseley SH Jr, Silverberg RF, Smoot GF, Weiss R, Wilkinson DT (1994) Measurement of the cosmic microwave background spectrum by the COBE FIRAS instrument. Astrophys J 420:439–444. doi:10.1086/173574
55. Moffat JW, Tatarski DC (1995) Cosmological observations in a local void. ApJ 453:17. doi:10.1086/176365. arXiv:astro-ph/9407036
56. Moroi T, Takahashi T (2001) Effects of cosmological moduli fields on cosmic microwave background. Phys Lett B 522:215–221. doi:10.1016/S0370-2693(01)01295-3. arXiv:hep-ph/0110096
57. Moroi T, Takahashi T (2002) Erratum to: "Effects of cosmological moduli fields on cosmic microwave background" [Phys. Lett. B 522 (2001) 215]. Phys Lett B 539:303–303. doi:10.1016/S0370-2693(02)02070-1
58. Moss A, Zibin JP, Scott D (2011) Precision cosmology defeats void models for acceleration. Phys Rev D 83(10):103515. doi:10.1103/PhysRevD.83.103515. arXiv:1007.3725
59. Mukhanov VF, Chibisov GV (1981) Quantum fluctuations and a nonsingular universe. Soviet J Exp Theor Phys Lett 33:532
60. Nadathur S, Sarkar S (2011) Reconciling the local void with the CMB. Phys Rev D 83(6):063506. doi:10.1103/PhysRevD.83.063506. arXiv:1012.3460
61. Particle Data Group (1998) Review of particle physics. Eur Phys J C3:1–794. doi:10.1007/s10052-998-0104-x. http://pdg.lbl.gov/1998/contents_large_sports.html
62. Peacock JA (1999) Cosmological physics. Cambridge University Press, Cambridge
63. Peebles PJE (1968) Recombination of the primeval plasma. ApJ 153:1. doi:10.1086/149628
64. Peebles PJE (1993) Principles of physical cosmology. Princeton University Press, New Jersey

65. Penzias AA, Wilson RW (1965) A measurement of excess antenna temperature at 4080 Mc/s. Astrophys J 142:419–421. doi:10.1086/148307
66. Pietronero L (1987) The fractal structure of the universe: correlations of galaxies and clusters and the average mass density. Phys A Stat Mech Appl 144:257–284. doi:10.1016/0378-4371(87)90191-9
67. Planck Collaboration (2014a) Planck 2013 results. XVI. Cosmological parameters. A&A 571:A16. doi:10.1051/0004-6361/201321591. arXiv:1303.5076
68. Planck Collaboration (2014b) Planck 2013 results. XXII. Constraints on inflation. A&A 571:A22. doi:10.1051/0004-6361/201321569. arXiv:1303.5082
69. Riess AG, Macri L, Casertano S, Lampeit H, Ferguson HC, Filippenko AV, Jha SW, Li W, Chornock R, Silverman JM (2011) A 3% solution: determination of the Hubble constant with the Hubble space telescope and wide field camera 3. ApJ 732:129. doi:10.1088/0004-637X/732/2/129
70. Robertson HP (1935) Kinematics and world-structure. ApJ 82:284. doi:10.1086/143681
71. Scharf CA, Jahoda K, Treyer M, Lahav O, Boldt E, Piran T (2000) The 2–10 keV X-ray background dipole and its cosmological implications. Astrophys J 544:49–62. doi:10.1086/317174. arXiv:astro-ph/9908187
72. Scrimgeour MI, Davis T, Blake C, James JB, Poole GB et al (2012) The WiggleZ Dark Energy Survey: the transition to large-scale cosmic homogeneity. MNRAS 425:116–134. doi:10.1111/j.1365-2966.2012.21402.x. arXiv:1205.6812
73. Seager S, Sasselov DD, Scott D (1999) A new calculation of the recombination epoch. Astrophys J Lett 523:L1–L5. doi:10.1086/312250. arXiv:astro-ph/9909275
74. Seery D, Lidsey JE (2005) Primordial non-Gaussianities from multiple-field inflation. J Cosmol Astropart Phys 9:011. doi:10.1088/1475-7516/2005/09/011. arXiv:astro-ph/0506056
75. Slipher VM (1913) The radial velocity of the Andromeda Nebula. Lowell Obs Bull 2:56–57
76. Slipher VM (1915) Spectrographic observations of Nebulae. Popul Astron 23:21–24
77. Starobinsky AA (1980) A new type of isotropic cosmological models without singularity. Phys Lett B 91:99–102. doi:10.1016/0370-2693(80)90670-X
78. Starobinsky AA (1982) Dynamics of phase transition in the new inflationary universe scenario and generation of perturbations. Phys Lett B 117:175–178. doi:10.1016/0370-2693(82)90541-X
79. Sylos LF, Vasilyev NL, Pietronero L, Baryshev YV (2009) Absence of self-averaging and of homogeneity in the large-scale galaxy distribution. In: [40], p 49001. doi:10.1209/0295-5075/86/49001. arXiv:0805.1132
80. Tomita K (2000) Distances and lensing in cosmological void models. ApJ 529:38–46. doi:10.1086/308277. arXiv:astro-ph/9906027
81. Verde L, Protopapas P, Jimenez R (2013) Planck and the local Universe: quantifying the tension. Phys Dark Universe 2:166–175. doi:10.1016/j.dark.2013.09.002. arXiv:1306.6766
82. Walker AG (1937) On milne's theory of world-structure. Proc Lond Math Soc S2 42(1):90–127. doi:10.1112/plms/s2-42.1.90. http://plms.oxfordjournals.org/content/s2-42/1/90.short. http://plms.oxfordjournals.org/content/s2-42/1/90.full.pdf+html
83. Wang FY, Dai ZG (2013) Testing the local-void alternative to dark energy using galaxy pairs. MNRAS 432:3025–3029. doi:10.1093/mnras/stt652. arXiv:1304.4399
84. Wu K, Lahav O, Rees M (1999) The large-scale smoothness of the Universe. Nature 397:225. doi:10.1038/16637. arXiv:astro-ph/9804062
85. Yadav APS, Wandelt BD (2010) Primordial non-gaussianity in the cosmic microwave background. Adv Astron. doi:10.1155/2010/565248. arXiv:1006.0275
86. Yoo CM, Nakao K, Sasaki M (2010) CMB observations in LTB universes. Part II: the kSZ effect in an LTB universe. J Cosmol Astropart Phys 10:011. doi:10.1088/1475-7516/2010/10/011. arXiv:1008.0469

87. York DG et al (2000) The sloan digital sky survey: technical summary. Astrophys J 120:1579–1587. doi:10.1086/301513. arXiv:astro-ph/0006396
88. Zhang P, Stebbins A (2011) Confirmation of the Copernican principle at Gpc radial scale and above from the kinetic Sunyaev-Zel'dovich effect power spectrum. Phys Rev Lett 107(4):041301. doi:10.1103/PhysRevLett.107.041301. arXiv:1009.3967
89. Zumalacárregui M, García-Bellido J, Ruiz-Lapuente P (2012) Tension in the void: cosmic rulers strain inhomogeneous cosmologies. J Cosmol Astropart Phys 10:009. doi:10.1088/1475-7516/2012/10/009. arXiv:1201.2790

http://www.springer.com/978-3-319-21881-6

The Intrinsic Bispectrum of the Cosmic Microwave Background

Pettinari, G.W.

2016, XXIII, 263 p. 21 illus., 19 illus. in color., Hardcover
ISBN: 978-3-319-21881-6